Evolutionary and plastic phenotypic change can be just as fast as changes in population densities

Guenchik Grosklos
Department of Mathematics and Statistics
Utah State University
Logan, UT 84322
guen.grosklos@aggiemail.usu.edu

Michael H. Cortez*
Department of Biological Science
Florida State University
Tallahassee, FL 32306
(850) 645-8692
mcortez@fsu.edu

November 4, 2020

Short running title: Comparing density and phenotypic rates
Keywords: Eco-evolutionary dynamics; fast-slow dynamical systems; rapid evolution; population dynamics; phenotypic plasticity; feedbacks
Article Submission
Abstract is 200 words; Main text is $\approx$ 5500 words
References: 74
Tables and Figures: 1 Table; 3 Figures; Figure 3 is color.
Supplementary Materials: (1) Author generated document. (2) Zip file uploaded to Dryad containing empirical data sets and Matlab scripts.
*Corresponding author
The authors wish to be identified to the reviewers

Abstract

Evolution and plasticity can drive population-level phenotypic change (e.g., changes in the mean phenotype) on time scales comparable to changes in population densities. However, it is unclear if phenotypic change has the potential to be just as fast as changes in densities, or if comparable rates of change only occur when densities are changing slow enough for phenotypes to keep pace. Moreover, it is unclear if this depends on the mode of adaptation. Using scaling theory and fast-slow dynamical systems theory, we develop a method for comparing maximum rates of density and phenotypic change estimated from population-level time series data. We apply our method to 30 published empirical studies where changes in morphological traits are caused by evolution, plasticity, or an unknown combination. For every study, the maximum rate of phenotypic change was 0.5 to 2.5 times faster than the maximum rate of change in density. Moreover, there were no systematic differences between systems with different modes of adaptation. Our results show that plasticity and evolution can drive phenotypic change just as fast as changes in densities. We discuss the implications of our results in terms of the strengths of feedbacks between population densities and traits.

Introduction

Populations change over time both in terms of their densities and in terms of the distributions of the phenotypes of individuals. The rate of phenotypic change at the population level (e.g., changes in the mean phenotype) and whether phenotypic change is driven by evolution versus plasticity can affect population-level dynamics, including species persistence following environmental change (Reed et al. 2011; Ghalambor et al. 2007) and invasion success (Lee 2002; Stockwell et al. 2003; Zenni et al. 2014). Empirical studies have shown that both evolution and plasticity have the potential to drive phenotypic change on the same time scale as changes in population densities. Studies on eco-evolutionary dynamics (Carrol et al. 2007; Fussman et al. 2007; Pelletier et al. 2009) have shown that evolution can occur fast enough to alter population dynamics over ecological time scales (e.g., a few generations). For example, rapid evolution during evolutionary rescue prevents species extinction driven by environmental change (Carlson et al. 2014; Bell 2017) and rapidly evolving prey defenses can cause and alter predator-prey cycles (Yoshida et al. 2003; 2007; Becks et al. 2010). Plastic behavioral and morphological response times can range between a few hours or a few weeks (Kuhlmann and Heckmann 1985; Kusch 1993; Auld and Relyea 2011; reviewed in Tollrian and Harvell 1999) and also can affect population dynamics (e.g., Verschoor et al. 2004; Lürling et al. 2005).

While these and other studies show that evolution and plasticity can drive population-level phenotypic change on the same time scale as changes in population densities, we might expect the relationships between density and phenotypic rates of change to systemically differ for plastic and evolving traits. In particular, it is reasonable to expect that phenotypic change is faster than changes in density (but still on the same time scale) for plastic responses that occur within the lifetime of an individual. In comparison, because evolutionary responses necessarily occur across generations, it is reasonable to expect that evolution would drive phenotypic change that is slower than changes in population densities (but also still on the same time scale). Thus, even though the changes in density and phenotypes are occurring

on similar time scales in both cases, we might expect the population-level rates of change for plastic traits to be faster than changes in population densities and the population-level rates of change for evolving traits to be slower than changes in population densities.

Understanding when phenotypic rates of change are faster than, equal to, or slower than changes in population densities is important because it, in part, determines the relative strengths of specific feedbacks, that in turn affect the dynamics of systems. Previous studies have focused on the roles ecological, evolutionary, and eco-evolutionary feedbacks play in driving eco-evolutionary dynamics (Cortez 2018; Patel et al. 2018; Fleischer et al. 2018; Cortez et al. 2020). These feedbacks can be naturally extended to density feedbacks (i.e., the effects species' densities have on the dynamics of population densities), phenotype feedbacks (i.e., the effects species' traits have on the dynamics of species traits), and density-phenotype feedbacks (i.e., the reciprocal effects densities and traits have on each other's dynamics). Importantly, all of the feedbacks affect the dynamics of a system, but a given feedback has relatively stronger effects when the involved variables change at faster rates and when the coupling between the variables is stronger (Patel et al. 2018; Cortez 2018); see appendix S1.1 for mathematical details. For example, if there is sufficient coupling between all densities and all phenotypes and species' densities change faster than phenotypes in a system, then theory predicts that effects of density feedbacks will be strongest, the effects of density-phenotype feedbacks will be intermediate, and the effects of phenotype feedbacks will be weakest. Thus, given sufficient coupling between densities and traits, feedbacks involving densities and traits with the fastest rates of change will have a stronger effect than feedbacks involving densities and traits with slower rates of change (Patel et al. 2018; Cortez 2018).

This suggests that if the relationships between density and phenotypic rates of change systemically differ for plastic and evolving traits, then different kinds of feedbacks have stronger effects on the dynamics of communities with plastic versus evolving traits. For example, if plastic traits change faster than population densities, then theory predicts that the effects of phenotype feedbacks are greater than the effects of density-phenotype feedbacks

which are greater than the effects of density feedbacks in those systems. In comparison, if evolving traits change slower than population densities, then theory predicts that the ordering is reversed in those systems (i.e., density feedbacks are strongest and phenotype feedbacks are weakest). Previous theoretical work on eco-evolutionary dynamics predicts that differences in the strengths of feedbacks and differences in the rates of density and phenotypic change can lead to different population-level dynamics in predator-prey and other communities (Vasseur et al. 2011; Patel and Schreiber 2015; Cortez 2016; van Velzen and Gaedke 2017; Cortez and Patel 2017; Cortez 2018). Thus, systematic differences in the relationships between density and phenotypic rates of change for plastic and evolving traits could imply different population-level dynamics in those systems.

A previous meta-analysis of empirical studies (DeLong et al. 2016) explored whether the rates of change of ecologically important phenotypes were faster, slower, or comparable to rates of change in densities. DeLong et al. (2016) found that average per capita rates of phenotypic change for both evolving and plastic traits were always slower than average per capita changes in density, with evolution being more than ten times slower in some cases. Based on the above, these results suggest that in all of those systems, density feedbacks were stronger than density-phenotype or phenotype feedbacks. However, this conclusion seems at odds with current mathematical theory for two reasons. First, eco-evolutionary theory for predator-prey systems (Cortez and Ellner 2010; Cortez 2016; van Velzen and Gaedke 2017) predicts that the cycle periods and phase lags observed in empirical systems with prey evolution (Yoshida et al. 2003; 2007; Becks et al. 2010; 2012) can only arise if prey evolution is sufficiently fast (which implies density-phenotype and phenotype feedbacks are sufficiently strong). Second, the body of mathematical theory that deals with the analysis of models with fast and slow variables (known as fast-slow dynamical systems theory; Arnold 1995; Kuehn 2015) does not define fast and slow variables in terms of average per capita rates of change. This suggests that additional work is needed to address the disagreement.

In this study, we explore how the mode of adaptation influences the relationships between

density and phenotypic rates of change in empirical systems. To do this, we develop a method for estimating and comparing rates of density and phenotypic change from empirical time series. Our method compares scaled maximum rates of change, a choice which is supported by two bodies of mathematical theory: fast-slow dynamical systems theory (Arnold 1995; Kuehn 2015) and scaling theory (Logan 2013). We apply our method to thirty published empirical studies with population-level time series of densities and morphological phenotypes. For all studies, we find that the maximum phenotypic rates of change are between 0.5 and 2.5 times faster than the maximum rates of change in population densities. Moreover, the relationships between density and phenotypic rates of change did not systemically differ for evolving and plastic traits. Our results suggest that both evolution and plasticity have the potential to drive phenotypic change that is just as fast as changes in densities (even though they may not always do so). We discuss the implications of our results in terms of the feedbacks that may be driving the dynamics in these systems.

Data sets, methods and theory

Estimating rates of change from empirical time series

We analyzed published time series from thirty empirical studies (Table 1), gathered from the seventeen studies analyzed in DeLong et al. (2016), searches using Web of Science and Google Scholar, and other studies known to the authors. A study was included if it contained population-level times series for density and a morphological trait from the same population. Data was either extracted from PDFs or provided by authors of the original study. All data sets and computational scripts are deposited in the Dryad Digital Repository: http://doi.org/10.5061/dryad.b5mkkwhb3 (Grosklos and Cortez 2020).

The thirty studies consist of seventeen field-based studies and thirteen constant condition laboratory experiments (FS and LE, respectively, in Table 1). In the field-based studies, temporal dynamics in densities and population-level phenotypes were driven by a combination

of species interactions and (natural) environmental forcing. In the laboratory experiments, the communities were held under constant environmental conditions, the communities were seeded with populations not at equilibrium densities or trait distributions, and temporal dynamics were driven by processes internal to the system (e.g., oscillations due to predator-prey interactions); see appendix S1.1 in the Supplementary Material for additional details.

In most studies, the phenotype of interest was a quantitative variable (e.g., beak length) and the population-level trait was the mean phenotype for the population. In eight of the studies, phenotypes were one of two qualitative types, e.g., susceptible or resistant strains of bacteria. In these systems, the proportion of individuals with a particular phenotype, e.g., proportion resistant, was used as the population-level trait. This is appropriate, because when individuals can only have one of two phenotypes, there is a one-to-one mapping between the mean trait value and the frequency of one phenotype; see appendix S1.1 in the Supplementary Material for details.

The mode of phenotypic change for each trait was classified as genetic, plastic, or an unknown combination (hereafter, unknown), based on measures of heritability or descriptions of the mode of adaptation in the original studies. 'Genetic' means either (i) the narrow sense heritability (h^2) of the trait measured from breeding experiments was estimated to be greater than 0.5 or (ii) the trait is for a clonal organism where plasticity was shown to be absent (e.g., prey expressing the undefended phenotype did not change expression in the presence of predators). 'Plastic' means that phenotypic plasticity was stated to be the known mode of phenotypic change (which could be shown, e.g., with reactions norms). The mode of adaptation for all other studies was classified as 'unknown'; this category includes traits whose narrow sense heritability was estimated less than 0.5 and traits where the mode of adaptation was unknown to the authors of the original study.

To determine whether rates of phenotypic change were faster, slower, or comparable to rates of change in population density in each system, we computed rates of change for each time series using finite differences and compared their scaled maximum magnitudes.

Specifically, given density values $\{x_1, x_2, ..., x_n\}$ at time points $\{t_1, t_2, ..., t_n\}$ and trait values $\{z_1, z_2, ..., z_m\}$ at time points $\{s_1, s_2, ..., s_m\}$, the scaled maximum rates of density and phenotypic change are

$$\begin{aligned} \epsilon_{den} &= \frac{G}{R_{den}} \max_i \left\{ \left| \frac{x_{i+1} - x_i}{t_{i+1} - t_i} \right| \right\} \\ \epsilon_{ph} &= \frac{G}{R_{ph}} \max_i \left\{ \left| \frac{z_{i+1} - z_i}{s_{i+1} - s_i} \right| \right\}. \end{aligned} \tag{1}$$

Here, the fractions in braces are the unscaled magnitudes of the rates of density and phenotypic change computed using finite differences; $R_{den} = \max\{x_i\} - \min\{x_i\}$ and $R_{ph} = \max\{z_i\} - \min\{z_i\}$ are the ranges of the density and phenotypic time series, i.e., the differences between the minimum and maximum values; and G is the generation time of the species. For studies with multiple time series, we computed ϵ_{den} and ϵ_{ph} for each time series and then computed average ϵ_{den} and ϵ_{ph} values.

When ϵ_{den} is larger than ϵ_{ph} ($\epsilon_{den} > \epsilon_{ph}$), the population density has the potential to change at rates faster than those possible for the population-level trait. Colloquially this means phenotypic change is slower than changes in densities. When ϵ_{den} is smaller than ϵ_{ph} ($\epsilon_{den} < \epsilon_{ph}$), the population-level trait has the potential to change at rates faster than those possible for the population density. Colloquially this means phenotypic change is faster than changes in densities. The justifications for this interpretation and our particular choice of scaling and comparison are presented in the following sections.

Distinguishing between fast and slow rates of change

In order to compare rates of change in population densities and population-level traits, we first need a way to define and distinguish between faster and slower variables (i.e., densities or traits). The body of mathematical theory that does this is fast-slow dynamical systems theory (Arnold 1995; Kuehn 2015). Below, we use that theory to show that (i) fast and slow

variables are defined by maximum rates of changes, (ii) faster variables have the potential to change much faster than slower variables but do not always do so, and (iii) the time series of fast and slow variables are distinguished by faster variables having larger maximum rates of change.

Fast-slow dynamical systems are models where some variables change much faster than others. They have been used to model plasticity (Cortez 2011) and eco-evolutionary dynamics (Dieckmann et al. 1995; Marrow et al. 1996; Khibnik and Kondrashov 1997; Dercole et al. 2006; Cortez and Ellner 2010). To introduce them, consider a minimal model for changes in the density (x) and population-level trait (z) of a species,

$$\begin{aligned} \frac{dx}{dt} &= \epsilon_x f(x,z) \\ \frac{dz}{dt} &= \epsilon_z g(x,z). \end{aligned} \tag{2}$$

The first equation defines how the population density changes due to all ecological processes, including interactions with other unmodeled species. The second equation describes how the population-level trait changes over time, e.g., due to selection or induction. The notation in model (2) is adapted from fast-slow systems theory and has the following biological interpretation. The values of ϵ_x and ϵ_z define the maximum magnitudes of the rates of density and phenotypic change, respectively. The functions f and g define the direction and the fraction of the maximum rate that the density or trait, respectively, is changing at. For example, $f(x,z) = 0.5$ and $g(x,z) = -1$ mean that the species' density is increasing at half of its maximum rate and the population-level trait is decreasing at its maximum rate. The magnitudes of ϵ_z and ϵ_x determine whether phenotypes have the potential to change at rates faster than those possible densities ($\epsilon_z > \epsilon_x$) or not ($\epsilon_z < \epsilon_x$). For example, $\epsilon_z/\epsilon_x = 2$ means that the population-level trait can change up to two times faster than the maximum rate of change in population density.

Fast-slow systems behave in the following way. The slow variable always changes at a

slow rate. In contrast, the fast variable has short periods of fast rates of change and long periods of slow rates of change. Figure 1 shows an example where density dynamics are fast and the phenotypic dynamics are much slower ($\epsilon_x = 1$ and $\epsilon_z = 0.01$). The population-level trait (z) always changes at a slow rate (dashed line close to 0 in Figure 1B). In contrast, the population density (x) changes at a fast rate whenever $f(x, z)$ is large in magnitude (solid line far from zero for $t \approx 0$ in Figure 1B). However, if $f(x, z)$ is small in magnitude, then dx/dt will be small and the population density will change at a slow rate (solid line near zero for large t in Figure 1B). The values of x and z that yield $f(x, z) = 0$ define the x-nullcline, which is known as the critical set in the fast-slow systems literature. When a solution to a fast-slow system is plotted in the phase portrait (Figure 1C), the fast variable has fast rates of change (double arrows) when away from the critical set (gray plane) and slow rates of change (single arrow) when near the critical set.

Importantly, because fast variables have time periods of both fast and slow rates of change, fast variables can be distinguished from slow variables only by comparing maximum rates of change. In particular, large and small maximum rates of change (ϵ_x, ϵ_z) define whether a variable is fast or slow, respectively. We make three points about this. First, a faster variable has the potential to change at much faster rates than a slower variable, but that does not mean that a faster variable is always changing at a fast rate. For example, prey density (the faster variable) in Figure 1B eventually changes as slowly as the prey trait (the slower variable). Second, a faster variable does not always change faster than a slower variable. In general, faster variables will change slower than slower variables whenever the rate of change in the faster variables is zero; this occurs whenever the variable passes through a local minimum or maximum value in the time series. For example, the phenotypic rate of change is faster at $t = 2$ in Figure 1B because prey density is at a trough.

Third, metrics that use different summary statistics can incorrectly classify fast variables as slow variables because fast variables spend much more time changing slowly, which ends up giving too little weight to the periods of time where fast changes are occurring. For example,

the average rates of phenotypic and density change in Figure 1B are nearly identical despite the phenotype being one hundred times slower than the population density. Overall, this shows that in order to determine if densities or phenotypes change faster, we need to compare the magnitudes of their maximum rates of change.

Scaling to account for units and dimensions of data

Now that we have a way to define fast and slow variables, we need a fair way to compare values estimated from time series of variables that are measured in different quantities (e.g., density versus length) and with different units (e.g., 1-2 cm versus 10-20 mm). This is done by scaling the variables such that they become dimensionless quantities; the body of mathematical theory that addresses this issue is known as scaling theory (Logan 2013). We note that scaling the species' densities and trait values changes the magnitudes of their rates of change and that this is necessary in order to be able to compare rates of change of quantities with different dimensions in an unbiased way. Below, we present our specific scaling and explain why it is a better choice than other possible scaling choices.

We scale the densities, phenotypes, and their rates of change by the range of each time series, i.e., the difference between the maximum and minimum values. We also scale the rates by the species' generation time, G, but because density and phenotypic rates for each species are scaled by the same value, our results are unchanged if a different value is used.

One key advantage of this scaling is that it removes biases caused by measuring the same quantity in different units. For example, if a species' mean body size is modeled as $100 + 10\sin(t)$ cm or, equivalently, $1 + 0.1\sin(t)$ m, then the rates of change are $10\cos(t)$ cm/yr and $0.1\cos(t)$ m/yr, respectively. The coefficients 10 and 0.1 correspond to ϵ_{ph} in model (1). This is a problem because the phenotype is classified as one hundred times faster in one case, even though the time series are identical after accounting for the different units. Dividing the rates of change by the range of the time series resolves this issue because both scaled rates become $0.5\cos(t)$ yr^{-1}.

The second key advantage of scaling by the range is that it avoids inconsistencies that arise with other scalings. Three alternative choices are to scale rates of change by (i) the maximum value of a variable, (ii) the value of the variable, or (iii) the sample standard deviation of the time series. As an illustrative example, consider two different populations whose mean beak lengths in each year (t) can be modeled as $\sin(t) + 2$ cm and $\sin(t) + 10$ cm. The rates of change in mean beak length are equal for both populations (both are $\cos(t)$ cm/yr) and scaling each by the range maintains the equivalence; both scaled rates are $0.5\cos(t)$ yr^{-1}. In contrast, scaling by the maximum value of a variable yields the unequal scaled rates $\cos(t)/3$ yr^{-1} and $\cos(t)/11$ yr^{-1}. Similarly, scaling by the value of the variable, i.e., using per capita rates of change, yields the unequal scaled rates $\cos(t)/[\sin(t) + 2]$ yr^{-1} and $\cos(t)/[\sin(t) + 10]$ yr^{-1}. Moreover, if a phenotype can take on a value of zero (e.g., spine length of zero), then the per capita rates of change can produce infinite values.

Scaling by the sample standard deviation avoids all of the above issues, but introduces additional issues. For example, consider a population whose mean beak length switches between 1 cm and 2 cm each year and a second population whose mean beak length is 2 cm every fifth year and 1 cm otherwise. When scaled by the range of the data, the scaled absolute maximum rates of change are correctly computed to be 1 for both populations. In contrast, when scaled by the standard deviation, the scaled maximum rates in the second population are always greater than the second due to the lower variation in the time series. In addition, in systems with fast and slow variables, the slow variable will often have lower variation than the fast variable because the slow variable can only change slowly. In these cases, scaling by the sample standard deviation ends up speeding up the slow variable and slowing down the fast variable, which then biases the results towards more equal rates of density and phenotypic change. In total, scaling the rates of change by the range of the variables avoids many inconsistencies introduced by alternative scalings.

Results

Application of Method to Simulated Data

To demonstrate that our method can identify when population densities change at faster or slower rates than population-level traits, we applied our method to simulations of the eco-evolutionary predator-prey model in Abrams and Matsuda (1997). To do this, we first chose parameter values such that the estimated maximum rates of density and phenotypic change taken from simulated time series were equal (i.e., ϵ_x and ϵ_z in the model were chosen such that the values of ϵ_{den} and ϵ_{ph} estimated from the simulated time series were equal). We then sped up (or slowed down) the rate of phenotypic change in the model by multiplying the right hand side of the trait equation (ϵ_z) by factors of 2, 0.5, 0.1, and 0.05, estimated the values of ϵ_{den} and ϵ_{ph} using our method, and compared the estimated values to the multiplicative factors set in the model. As shown in Figure 2A, our method captures how the phenotypic rates were sped up or slowed down. Specifically, as we decreased the maximum phenotypic rate in the model, our method showed a transition from maximum phenotypic rates being faster than (triangle; Figure 2B) to being equal to (asterisk; Figure 2C) to being slower than (x, square, and circle; Figure 2D) maximum rates of change in density. Additionally, the estimated maximum density rate remained unchanged, which is consistent with how the speed of the population dynamics was unaltered in the model.

We note that the estimated values of ϵ_{ph} are not identical to the values used in the model. For example, $\epsilon_z = 0.05\epsilon_x$ in the model for the simulation with the slowest rate of phenotypic change, but the estimated value of ϵ_{ph} is $0.066\epsilon_{den}$. This difference is not surprising because each time series has a different range and is therefore scaled by a different numerical value. The ranges differ because the system is stabilized as the maximum rate of phenotypic change decreases (sustained cycles occur in Figure 2B while convergence to equilibrium occurs in Figure 2C,D). This is not an issue when applying our method to the empirical data sets because we are not comparing rates of density or phenotypic change

between different empirical systems (where ranges of the variables differ). Instead, we are only comparing the rate of phenotypic change to the rate of density change for the same empirical system.

One limitation of our method is that the estimated maximal rates of change ($\epsilon_{den}, \epsilon_{ph}$) depend on the sampling interval of the time series (i.e., the length of time between consecutive data points). In general, larger sampling intervals lead to scaled maximum rates of change that are close to 1. In addition, the magnitude of the effect is larger for variables with greater variation (which often means variables with faster rates of change). For example, Figure 2F-H shows how increasing the sampling interval affects the time series in panels B-D. For all of the time series in Figure 2A, increases in the sampling interval move the estimated scaled maximum rates of change closer to the one-to-one line (light gray shapes in Figure 2 are closer to one-to-one line than black shapes). The main implication for our results is that if the sampling is too sparse, our results will be biased towards concluding that the scaled maximum rates of density and phenotypic change are more similar than in reality.

Application of Method to Empirical Time Series

We applied our method for estimating maximum rates of density and phenotypic change to the 30 published studies (Table 1); see Table S1 and the supplementary material for additional details. Across all studies, we found that the maximum rate of phenotypic change was between 0.5 and 2.5 times faster than the maximum rate of density change; the mean and median were 1.2 and the lower and upper quartiles were 0.85 and 1.5, respectively. Additionally, in only three studies did the maximum scaled rates differ by more than a factor of two (three studies above upper dashed lines in Figure 3A,B). The mode of adaptation did not affect the relationship between the maximum rates (Figure 3B); rates of phenotypic change were faster than rates of density change in approximately half of the studies in each category. Overall, our results suggest that population densities and population-level phenotypes could change at similar rates in all systems and that the mode of adaptation did

not have an effect on the relationship between rates of density and phenotypic change.

Sparse sampling can potentially bias our results toward estimating equal maximum scaled rates of density and phenotypic change. Many of the study systems satisfy conditions that suggest undersampling is less likely to be an issue; see appendix S1.1 in the Supplementary Material for additional details. For 17 of the 30 studies, the average sampling interval is less than or equal to the species' generation time (Figure S2). This suggests that for those 17 studies, undersampling is unlikely to bias our results. In 6 of the 13 studies where the sampling interval is greater than the species' generation time, the adapting species is the prey species in an oscillating predator-prey system. Because the predator generation time imposes limits on the cycle period and the sampling interval is less than the predator generation time, undersampling is unlikely to bias our results for those 6 studies. Undersampling may be an issue for 3 studies with genetic traits (Bohannon and Lenski 1998; Sanchez and Gore 2013; Schrag and Mittler 1996) and 4 studies with plastic traits (Caron et al. 1985; DeLong et al. 2014; Gonzalez et al. 1993; Suzuki et al. 2017) where the sampling interval is greater than the species' generation time.

Discussion

In this study, we compared scaled maximum rates of density and phenotypic change in thirty empirical studies and found that phenotypic rates range from 0.5 to 2.5 times faster than rates of change in population density. Moreover, we found that the relationship between rates of density and phenotypic change did not differ for systems with plastic versus evolving morphological traits. Overall, our results show that plasticity and evolution have the potential to drive changes in morphological traits that are just as fast as changes in population densities. On the one hand, our general findings are not surprising given that there are many empirical studies documenting evolution occurring on ecological time scales (e.g., Carrol et al. 2007; Fussman et al. 2007; Pelletier et al. 2009) and plastic responses in individuals

can occur within hours or weeks (e.g., Kuhlmann and Heckmann 1985; Kusch 1993; Auld and Relyea 2011). On the other hand, our results are somewhat unexpected because evolutionary change necessarily requires multiple generations whereas all of the plastic responses in the studies we considered occur within the lifetime of the organism. Our results suggest that this difference did not have a strong effect on the relationships between population-level rates of change in densities and phenotypes for the studies we analyzed.

Our main conclusion is that plasticity and evolution have the potential to drive population-level changes in morphological traits that are just as fast as changes in population densities. Our use of the word 'potential' is intentional, because our results do not mean that rates of density and phenotypic change are always comparable. Rapid phenotypic change occurs for evolving traits when there is strong selective pressure and high genetic variation and for plastic traits when rates of induction or loss of induction are high. Rapid changes in densities can occur when a species' interactions with its environment (e.g., intraspecific and interspecific interactions with other species) are strong. In general, we do not expect the conditions for rapid phenotypic change and rapid changes in density to align in time. This means that we expect to observe periods of time where rates of phenotypic change are greater than rates of change in densities, and vice versa. Thus, overall our results support the claim that phenotypic change can be just as fast as evolutionary change.

One caveat to our conclusions is that we only focused on plastic morphological phenotypes that change within the lifetime of the organism. Our conclusions may extend to transgenerational plastic responses, wherein an offspring's phenotype is determined by the parent's environment (Agrawal et al. 1999; Shimada et al. 2010). This is because the generational lag in such plastic responses is similar to the lag for evolutionary responses. However, we do not expect that our results will extend to all behavioral responses. Behavioral plastic responses can occur over periods of time much shorter than the generation time of the organism (Tollrian and Harvell 1999). For such traits, it seems virtually guaranteed that population-level changes in phenotypes can be much faster than changes in population densities.

Our results differ markedly from DeLong et al. (2016), who found that evolutionary or plastic phenotypic change was no more than two-thirds as fast as changes in population densities. Our method and the method in DeLong et al. (2016) use different scalings (range of the data versus per capita rates) and compare different values (maximum rates versus average rates). Our comparison of these two approaches in Figure S3 of appendix S1.4 in the Supplementary Material shows that the difference in scaling is the key factor causing the differing results. Specifically, our results are nearly identical if we compare average rates of change scaled by the range of the time series. Our results are also nearly identical if we compare maximum or average rates of change scaled by the sample standard deviation of the time series; see Figure S3. We have argued that our method is better than the alternatives because it is consistent with fast-slow dynamical systems theory and scaling theory and because it avoids inconsistencies that arise with other methods. Our comparison of methods suggests that the issues associated with using average rates of change or scaling by the sample standard deviation are not present in our data sets. However, it also suggests that the issues associated with using per capita rates are. This is not surprising since the trait values and densities take on small values in many of the studies, which can lead to errors when computing per capita rates. In total, while other methods can yield similar results, we recommend comparing maximum rates of change that are scaled by the range of the data in order to avoid potential errors.

Finally, our results suggest that multiple types of feedbacks were likely important for driving the dynamics in the systems we considered. The strengths of density feedbacks (i.e., feedbacks between population densities), phenotype feedbacks (i.e., feedbacks between species traits), and density-phenotype feedbacks (i.e., feedbacks between population densities and species traits) depend on the coupling between the variables involved in the feedback and by how fast the variables can change (ϵ_{den} and ϵ_{ph} in our study) (Patel et al. 2018; Cortez 2018). Because we focused on studies with changes in ecologically relevant traits, the coupling between densities and traits was likely high. Given this sufficient coupling,

the similarity in density and phenotypic rates of change suggests that density, phenotype, and density-phenotype feedbacks were roughly equally strong in all systems. This relates to previous empirical (Yoshida et al. 2003; 2007; Becks et al. 2010; Verschoor et al. 2004; Steiner and Masse 2013) and theoretical (Cortez 2011) studies that suggest plasticity and evolution have different effects on the population dynamics of predator-prey systems. If our results about rates of density and phenotypic change are generally true for predator-prey systems, then this would suggest that dynamical differences between predator-prey systems with plastic and evolving traits might not be due to which feedbacks are driving the dynamics, but instead due to differences between the properties of the feedbacks involving plastic versus evolving traits (e.g., stabilizing versus destabilizing feedbacks).

More generally, it is currently not known if and how the feedbacks involving plastic versus evolving traits differ. This points to a need for new theory that directly compares the feedbacks between evolving traits and population densities with the feedbacks between plastic traits and densities. Much of the current theoretical work on systems with evolving or plastic traits assumes phenotypic rates of change are either much slower (e.g., Marrow et al. 1996; Dercole et al. 2006; Patel et al. 2018) or much faster (e.g., Cortez and Ellner 2010; Cortez 2011; Patel et al. 2018) than density rates of change. In these systems, density feedbacks are much stronger than phenotype feedbacks, or vice versa. However, our results suggest that density feedbacks and phenotype feedbacks may be equally strong in many systems. Recent eco-evolutionary theory (Cortez 2016; Patel et al. 2018; Cortez 2018) shows that theory assuming very fast or very slow rates of phenotypic change may not accurately predict the dynamics of systems with comparable rates of density and phenotypic change. Thus, the results in our study point to the need for new theory that explains how feedbacks between densities and traits affect the dynamics of natural communities with commensurate rates of density and phenotypic change.

Acknowledgements

We thank David Vasseur and two anonymous reviewers for suggestions and helpful comments. We thank L Becks, E Edeline, SP Ellner, M Kasada, and A Sanchez for sharing empirical data sets with us. GG received support from the National Science Foundation under Grant No. 1633756.

Author Contributions

MHC designed research. GG performed research and analyzed data sets. GG and MHC wrote the paper.

References

Abrams, P. A., and H. Matsuda. 1997. Prey adaptation as a cause of predator-prey cycles. Evolution 51:1742–1750.

Agrawal, A. A., C. Laforsch, and R. Tollrian. 1999. Transgenerational induction of defences in animals and plants. Nature 401:60–63.

Jones, C. K. R. T. 1995. Geometric Singular Perturbation Theory. Pages 44–118 in Johnson, R. ed. Dynamical Systems. Lecture Notes in Mathematics, vol 1609. Springer, Berlin, Heidelberg.

Auld, J. R., and R. A. Relyea. 2011. Adaptive plasticity in predator-induced defenses in a common freshwater snail: altered selection and mode of predation due to prey phenotype. Evolutionary Ecology 25:189–202.

Becks, L., S. Ellner, L. E. Jones, and N. G. Hairston Jr. 2012. Reduction of adaptive genetic diversity radically alters eco-evolutionary community dynamics. Ecology Letters 13:989–997.

Becks, L., S. P. Ellner, L. E. Jones, and N. G. Hairston Jr. 2010. The functional genomics of an eco-evolutionary feedback loop: linking gene expression, trait evolution, and community dynamics. Ecology Letters 15:492–501.

Bell, G. 2017. Evolutionary rescue. Annual Review of Ecology, Evolution, and Systematics 48:605–627.

Bohannon, B. J. M., and R. E. Lenski. 1998. Effect of prey heterogeneity on the response of a model food chain to resource enrichment. American Naturalist 153:73–82.

Brown, C. R., and M. B. Brown. 2013. Where has all the road kill gone? Current Biology 23:R233–R234.

Campbell, T., and A. Echternacht. 2003. Introduced species as moving targets: changes in body sizes of introduced lizards following experimental introductions and historical invasions. Biological Invasions 5:193–212.

Carlson, S. M., J. Cunningham, and P. A. Westley. 2014. Evolutionary rescue in a changing world. Trends in Ecology and Evolution 29:521–530.

Caron, D. A., J. C. Goldman, O. K. Andersen, and M. R. Dennett. 1985. Nutrient cycling in a microflagellate food chain: Ii. population dynamics and carbon cycling. Marine Ecology Progress Series 24:243–254.

Carrol, S. P., A. P. Hendry, D. N. Reznick, and C. W. Fox. 2007. Evolution on ecological time-scales. Functional Ecology 21:387–393.

Coltman, D. W., P. O'Donoghue, J. T. Jorgenson, J. T. Hogg, C. Strobeck, and M. Festa-Bianchet. 2003. Undesirable evolutionary consequences of trophy hunting. Nature 426:655–658.

Cortez, M., and S. Ellner. 2010. Understanding rapid evolution in predator-prey interactions using the theory of fast-slow dynamical systems. American Naturalist 176:E109–E127.

Cortez, M. H. 2011. Comparing the qualitatively different effects rapidly evolving and rapidly induced defences have on predator-prey interactions. Ecology Letters 14:202–209.

Cortez, M. H. 2016. How the magnitude of prey genetic variation alters predator-prey eco-evolutionary dynamics. American Naturalist 188:329–341.

Cortez, M. H. 2018. Genetic variation determines which feedbacks drive and alter predator-prey eco-evolutionary cycles. Ecological Monographs 88:353–371.

Cortez, M. H., and S. Patel. 2017. The effects of predator evolution and genetic variation on predator-prey population-level dynamics. Bulletin of Mathematical Biology 79:1510–1538.

Cortez, M. H., S. Patel, and S. J. Schreiber. 2020. Destabilizing evolutionary and eco-evolutionary feedbacks drive empirical eco-evolutionary cycles. Proceedings of the Royal Society B 287:20192298.

DeLong, J. P., V. E. Forbes, N. Galic, J. P. Gibert, R. G. Laport, J. S. Phillips, and J. M. Vavra. 2016. How fast is fast? Eco-evolutionary dynamics and rates of change in populations and phenotypes. Ecology and Evolution 6:573–581.

DeLong, J. P., T. C. Hanley, and D. A. Vasseur. 2014. Predator–prey dynamics and the plasticity of predator body size. Functional Ecology 28:487–493.

Dercole, F., R. Ferriére, A. Gragnani, and S. Rinaldi. 2006. Coevolution of slow-fast populations: evolutionary sliding, evolutionary pseudo-equilibria and complex Red Queen dynamics. Proceedings of the Royal Society B 273:983–990.

Dieckmann, U., P. Marrow, and R. Law. 1995. Evolutionary cycling in predator-prey interactions: population dynamics and the Red Queen. Journal of Theoretical Biology 176:91–102.

Edeline, E., T. B. Ari, L. A. Vø llestad, I. J. Winfiled, J. M. Fletcher, J. B. James, and

N. C. Stenseth. 2008. Antagonistic selection from predators and pathogens alters food-web structure. PNAS 105:19792–19796.

Ezard, T. H. G., S. D. Cô té, and F. Pelletier. 2009. Eco-evolutionary dynamics: disentangling phenotypic, environmental and population fluctuations. Philosophical Transactions of the Royal Society B 364:1491–1498.

Fenchel, T., and P. R. Jonsson. 1988. The functional biology of strombidium sulcatum, a marine oligotrich ciliate (ciliophora, oligotrichina). Marine Ecology Progress Series 48:1–15.

Fischer, B. B., M. Kwiatkowski, M. Ackermann, J. Krismer, S. Roffler, M. J. Suter, R. I. Eggen, and B. Matthews. 2014. Phenotypic plasticity influences the eco-evolutionary dynamics of a predator–prey system. Ecology 95:3080–3092.

Fleischer, S. R., C. P. terHorst, and J. Li. 2018. Pick your trade-offs wisely: Predator-prey eco-evo dynamics are qualitatively different under different trade-offs. Journal of Theoretical Biology 456:201–212.

Fussman, G. F., S. P. Ellner, and N. G. Hairston Jr. 2003. Evolution as a critical component of plankton dynamics. Proceedings of the Royal Society of London B 270:1015–1022.

Fussman, G. F., M. Loreau, and P. A. Abrams. 2007. Eco-evolutionary dynamics of communities and ecosystems. Functional Ecology 21:465–477.

Ghalambor, C. K., J. K. McKay, S. P. Carroll, and D. N. Reznick. 2007. Adaptive versus non-adaptive phenotypic plasticity and the potential for contemporary adaptation in new environments. Functional Ecology 21:394–407.

Gonzalez, J. M., E. Sherr, and B. F. Sherr. 1993. Differential feeding by marine flagellates on growing versus starving, and on motile versus nonmotile, bacterial prey. Marine Ecology Progress Series 102:257–267.

Grant, P. R., and B. R. Grant. 2002. Unpredictable evolution in a 30-year study of Darwin's finches. Science 296:707–711.

Grosklos, G., and M.H.. Cortez. 2020. Data from: Evolutionary and plastic phenotypic change can be just as fast as changes in population densities. American Naturalist, Dryad Digital Repository, http://doi.org/10.5061/dryad.b5mkkwhb3 .

Haafke, J., M. A. Chakra, and L. Becks. 2016. Eco-evolutionary feedback promotes Red Queen dynamics and selects for sex in predator populations. Evolution 70:641–652.

Hiltunen, T., and L. Becks. 2014. Consumer co-evolution as an important component of the eco-evolutionary feedback. Nature Communications 5:1–8.

Hiltunen, T., S. P. Ellner, G. Hooker, L. E. Jones, and N. G. Hairston Jr. 2014. Eco-evolutionary dynamics in a three-species food web with intraguild predation: intriguingly complex. Advances in Ecological Research 50:41–73.

Kasada, M., M. Yamamichi, and T. Yoshida. 2014. Form of an evolutionary tradeoff affects eco-evolutionary dynamics in a predator-prey system. PNAS 111:16035–16040.

Khibnik, A., and A. Kondrashov. 1997. Three mechanisms of Red Queen dynamics. Philosophical Transactions of the Royal Society B: Biological Sciences 264:1049–1056.

Kuehn, C. 2015. Multiple time scale dynamics. Springer, Berlin.

Kuhlmann, H., and K. Heckmann. 1985. Interspecific morphogens regulating prey-predator relationships in protozoa. Science 227:1347–1349.

Kusch, J. 1993. Behavioural and morphological changes in ciliates induced by the predator *amoeba proteus*. Oecologia 96:354–459.

Le Galliard, J.-F., P. S. Fitze, R. Ferrière, and J. Clobert. 2005. Sex ratio bias, male aggression, and population collapse in lizards. PNAS 102:18231–18236.

Lee, C. E. 2002. Evolutionary genetics of invasive species. Trends in Ecology and Evolution 17:386–391.

Logan, D. J. 2013. Applied Mathematics. Wiley, Hoboken, New Jersey.

Lürling, M., H. Arends, W. Beekman, M. Vos, I. Van der Stap, W. Mooij, and M. Scheffer. 2005. Effect of grazer-induced morphological changes in the green alga scenedesmus obliquus on growth of the rotifer brachionus calyciflorus. Internationale Vereinigung für theoretische und angewandte Limnologie: Verhandlungen 29:698–703.

Marrow, P., U. Dieckmann, and R. Law. 1996. Evolutionary dynamics of predator-prey systems: an ecological perspective. Journal of Mathematical Biology 34:556–578.

Milot, E., F. M. Mayer, D. H. Nussey, M. Boisvert, F. Pellletier, and D. Ré ale. 2011. Evidence for evolution in response to natural selection in a contemporary human population. PNAS 108:17040–17045.

Nakazawa, T., N. Ishida, M. Kato, and N. Yamamura. 2007. Larger body size with higher predation rate. Ecology of Freshwater Fish 16:362–372.

Ozgul, A., D. Z. Childs, M. K. Oli, K. B. Armitage, D. T. Blumstein, L. E. Olson, S. Tuljapurkar, and T. Coulson. 2010. Coupled dynamics of body mass and population growth in response to environmental change. Nature 466:482.

Ozgul, A., S. Tuljapurkar, T. G. Benton, J. M. Pemberton, T. H. Clutton-Brock, and T. Coulson. 2009. The dynamics of phenotypic change and the shrinking sheep of St. Kilda. Science 325:464–467.

Patel, S., M. H. Cortez, and S. J. Schreiber. 2018. Partitioning the effects of eco-evolutionary feedbacks on community stability. American Naturalist 191:381–394.

Patel, S., and S. J. Schreiber. 2015. Evolutionary-driven shifts in communities with intraguild predation. American Naturalist 186:E98–E110.

Pelletier, F., D. Garant, and A. Hndry. 2009. Eco-evolutionary dynamics. Philosophical Transactions of the Royal Society B 364:1483–1489.

Reed, T. E., D. E. Schindler, and R. S. Waples. 2011. Interacting effects of phenotypic plasticity and evolution on population persistence in a changing climate. Conservation Biology 25:56–63.

Robinson, M. R., J. G. Pilkington, T. H. Clutton-Brock, J. M. Pemberton, and L. E. B. Kruuk. 2006. Live fast, die young: trade-offs between fitness components and sexually antagonistic selection on weaponry in soay sheep. Evolution 60:2168–2181.

Sanchez, A., and J. Gore. 2013. Feedback between population and evolutionary dynamics determines the fate of social microbial populations. PLoS Biology 11:e1001547.

Schoener, T. W., D. A. Spiller, and J. B. Losos. 2002. Predation on a common anolis lizard: can the food-web effects of a devastating predator be reversed? Ecological Monographs 72:383–407.

Schrag, S. J., and J. E. Mittler. 1996. Host-parasite coexistence: the role of spatial refuges in stabilizing bacteria-phage interactions. American Naturalist 148:348–377.

Shimada, M., Y. Ishii, and H. Shibao. 2010. Rapid adaptation: a new dimension for evolutionary perspectives in ecology. Population Ecology 52:5–14.

Sinervo, B., E. Svensson, and T. Comendant. 2000. Density cycles and an offspring quantity and quality game driven by natural selection. Nature 406:985–988.

Steiner, C. F., and J. Masse. 2013. The stabilizing effects of genetic diversity on predator-prey dynamics. F1000Research 2:43.

Stockwell, C. A., A. P. Hendry, and M. T. Kinnison. 2003. Contemporary evolution meets conservation biology. Trends in Ecology and Evolution 18:94–101.

Suzuki, K., Y. Yamauchi, and T. Yoshida. 2017. Interplay between microbial trait dynamics and population dynamics revealed by the combination of laboratory experiment and computational approaches. Journal of Theoretical Biology 419:201–210.

Swain, D. P., A. F. Sinclair, and J. M. Hanson. 2007. Evolutionary response to size-selective mortality in an exploited fish population. Proceedings of the Royal Society B: Biological Sciences 274:1015–1022.

Tessier, A., A. Young, and M. Leibold. 1992. Population dynamics and body-size selection in *Daphnia*. Limnology and Oceanography 37:1–13.

Tollrian, R., and C. D. Harvell. 1999. The Ecology and Evolution of Inducible Defenses. Princeton University Press, Princeton, NJ.

van Velzen, E., and U. Gaedke. 2017. Disentangling eco-evolutionary dynamics of predator-prey coevolution: the case of antiphase cycles. Scientific Reports 7.

Vasseur, D. A., P. Amarasekare, V. H. W. Rudolf, and J. M. Levine. 2011. Eco-evolutionary dynamics enable coexistence via neighbor-dependent selection. American Naturalist 178:E96–E109.

Verschoor, A. M., M. Vos, and I. van der stap. 2004. Inducible defences prevent strong population fluctuations in bi- and tritrophic food chains. Ecology Letters 7:1143–1148.

Yoshida, T., S. P. Ellner, L. E. Jones, B. J. M. Bohannon, R. E. Lenski, and N. G. Hairston. 2007. Cryptic population dynamics: rapid evolution masks trophic interactions. PLoS Biology 5:1–12.

Yoshida, T., L. E. Jones, S. P. Ellner, G. F. Fussman, and N. G. Hairston. 2003. Rapid evolution drives ecological dynamics in a predator-prey system. Nature 424:303–306.

Zenni, R. D., J.-B. Lamy, L. J. Lamarque, and A. J. Porté. 2014. Adaptive evolution and

phenotypic plasticity during naturalization and spread of invasive species: implications for tree invasion biology. Biological Invasions 16:635–644.

Tables

Table 1: Estimated scaled maximum rates of density and phenotypic change from empirical studies

Mode of Adaptation	Code	Study	Type	Species	Trait	ϵ_{den}	ϵ_{ph}
Genetic							
	a	Becks et al. (2010)	LE	*Chlamydomonas reinhardtii*	Clump size	0.37	0.63
	b	Becks et al. (2012)	LE	*Chlamydomonas reinhardtii*	Clump size	2.5	4.8
	c	Bohannon and Lenski (1998)	LE	*Escherichia coli*	Proportion susceptible	0.0097	0.012
	d	Coltman et al. (2003)	FS	*Ovis canadensis*	Horn length (adult male)	1.8	2.4
	e	Fussman et al. (2003)	LE	*Brachionus calyciflorous*	Proportion mictic (female)	0.97	1.8
	f	Grant and Grant (2002)	FS	*Geospiza fortis*	Beak length	2.9	2.1
	g		FS		Beak shape	2.9	1.9
	h	Grant and Grant (2002)	FS	*Geospiza scandens*	Beak length	2	1.9
	i		FS		Beak shape	2	1.1
	j	Haafke et al. (2016)	LE	*Chlamydomonas reinhardtii*	Clump size	0.055	0.076
	k	Hiltunen and Becks (2014)	LE	*Pseudomonas flourescens*	Proportion defended	0.43	0.23
	l	Hiltunen et al. (2014)	LE	*Chlorella autotrophica*	Clump size	0.16	0.38
	m	Kasada et al. (2014)	LE	*Chlorella vulgaris*	Proportion defended (costly tradeoff)	0.43	0.43
	n		LE		Proportion defended (cheap tradeoff)	0.82	0.57
	o	Milot et al. (2011)	FS	*Homo sapiens*	Age at first reproduction	0.58	0.77
	p	Robinson et al. (2006)	FS	*Ovis aries*	Proportion normal horned	2.7	6.1
	q	Sanchez and Gore (2013)	LE	*Saccharomyces cerevisiae*	Proportion cooperator	0.039	0.081
	r	Schrag and Mittler (1996)	LE	*Escherichia coli*	Proportion resistant	0.28	0.17
Plastic							
	A	Campbell and Echternacht (2003)	FS	*Anolis sagrei*	Snout-vent length	0.51	0.78
	B	Caron et al. (1985)	LE	*Paraphysomonas imperforata*	Cell volume	0.22	0.21
	C	DeLong et al. (2014)	LE	*Didinium*	Cell volume	0.11	0.14
	D	Fenchel and Jonsson (1988)	LE	*Strombidium sulcatum*	Cell volume	1.7	2.5
	E	Gonzalez et al. (1993)	LE	*Cafeteria* sp.	Cell volume	0.26	0.22
	F	Lürling et al. (2005)	LE	*Scenedesmus obliquus*	Clump size	0.53	0.39
	G	Ozgul et al. (2010)	FS	*Marmota flaviventris*	Weight	1.7	3.1
	H	Suzuki et al. (2017)	LE	*Flectobacillus*	Cell volume	0.023	0.017
Unknown							
	α	Brown and Brown (2013)	FS	*Petrochelidon pyrrhonotanest*	Wing length	0.69	0.59
	β	Coltman et al. (2003)	FS	*Ovis canadensis*	Weight (adult male)	1.8	2.8
	γ	Edeline et al. (2008)	FS	*Perca fluviatilis*	Body length	2.3	3.6
	δ	Ezard et al. (2009)	FS	*Ovis aries*	Weight	4.3	5.6
	η	Fischer et al. (2014)	LE	*Chlamydomonas reinhardtii*	Proportion strain 1	0.22	0.27
	θ	Nakazawa et al. (2007)	FS	*Gymnogobius isaza*	Body length	0.72	0.69
	λ		FS		Wet weight	0.72	0.79
	μ	Schoener et al. (2002)	FS	*Anolis sagrei*	Hindlimb length	0.81	0.69
	ξ		FS		Lamellae number	0.81	0.97
	ρ	Sinervo et al. (2000)	FS	*Uta stansburiana*	Clutch size	0.62	0.72
	σ		FS		Egg mass	0.62	0.87
	τ		FS		Proportion orange-throated (female)	0.61	0.96
	ϕ	Swain et al. (2007)	FS	*Gadus morhua*	Body length at age 6 years	1.5	1.4
	ψ	Tessier et al. (1992)	FS	*Daphnia galeata mendotae*	Body size	3.7	3

Mode of adaptation is either genetic (a−r), plastic (A−H), or unknown ($\alpha - \psi$). Study type is either field-based study (FS) or laboratory experiment under controlled conditions (LE); see text for details. The values ϵ_{den} and ϵ_{ph} are the scaled maximum rates of density and phenotypic change, respectively.

Figure captions

Figure 1: Behavior of a fast-slow eco-evolutionary predator-prey model where evolution of prey defense is slow. (A) Prey density (solid black) and mean prey defense (dashed black); predator density is not shown. (B) Rates of change for prey density (solid black) and mean defense (dashed black). The vertical dashed line denotes where rates of change in prey density transition from being faster than (left) to similar to (right) phenotypic rates of change. (C) Solution (solid black line) plotted in phase space with the critical manifold (gray). Double and single arrows denote when rates of change in population density are much faster than and similar to, respectively, rates of phenotypic change. Simulation is of the Abrams and Matsuda (1997) model; see appendix S1.3 in the Supplementary Material for equations and parameter values.

Figure 2: With sufficient sampling, our method can accurately estimate maximum rates of density and phenotypic change from simulated time series generated. Time series were generated using the eco-evolutionary predator-prey model in Abrams and Matsuda (1997), where the rate of evolution was sped up or slowed down by factors of 2, 1, 0.5, 0.1, and 0.05. (A) Estimated scaled maximum rates of density and phenotypic change for different speeds of evolution. Diagonal lines denote when maximum rates of phenotypic change are ten times faster (upper dashed line), equal to (solid line), and ten times slower (lower dashed line) than maximum rates of change in population densities. Examples of scaled prey density (solid black) and mean trait (dashed black) time series when (B) $\epsilon_{ph} \approx 2\epsilon_{den}$, (C) $\epsilon_{ph} \approx \epsilon_{den}$, and (D) $\epsilon_{ph} \approx 0.1\epsilon_{den}$. (E) Estimated scaled maximum rates of density and phenotypic change for different speeds of evolution and sampling intervals. Sampling is every 1 (black shapes), 4, 10, 20, 40, 100 or 200 (lightest gray shapes) time units. (F-H) Demonstration of how increasing the sampling interval to every 40 time steps alters the time series in panels B-D; numerical values differ between pairs of panels because the sampling interval affects the range of the time series and consequently, how each time series is scaled. See appendix S1.3 in the Supplementary Material for model equations and parameter values.


range_scaled_maximum_results_and_avg_modes-eps-converted-to.pdf

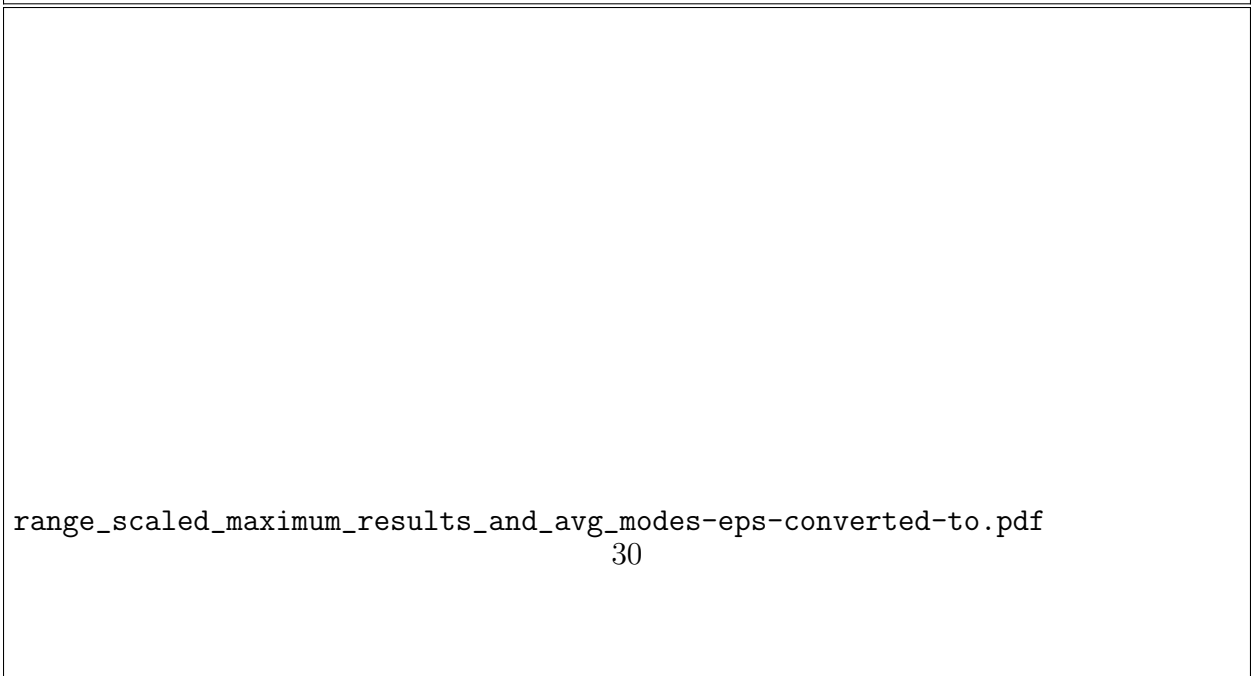
range_scaled_maximum_results_and_avg_modes-eps-converted-to.pdf

Supplementary Material for 'Evolution and plastic phenotypic change can be just as fast as changes in population densities'
American Naturalist

Guenchik Grosklos[1] and Michael H. Cortez[2]

[1]Department of Mathematics and Statistics, Utah State University, Logan, UT 84322

[2]Department of Biological Science, Florida State University, Tallahassee, FL 32306

mcortez@fsu.edu

Contents

S1.1 The link between feedbacks and rates of change

Here, we show how the rates of density and phenotypic change affect the strengths of density, density-phenotype, and phenotype feedbacks. Density feedbacks are the effects species' densities have on the dynamics of population densities, phenotype feedbacks are the effects species' traits have on the dynamics of species traits, and density-phenotype feedbacks are reciprocal between species' population densities and traits.

Mathematically, the presence/absence of these feedbacks is determined by how the rates of change depend on the variables, i.e., the coupling between the variables. To illustrate this, let x and z be the density and population-level phenotype of a species with dynamics $dx/dt = \epsilon_x f(x,z)$ and $dz/dt = \epsilon_z g(x,z)$, respectively, where ϵ_x and ϵ_z are the maximum rates of phenotypic change and $-1 \leq f, g \leq 1$; see the section "*Distinguishing between fast and slow rates of change*" in the main text for more details. A density feedback is present if the density dynamics depends on the density of the species, i.e., $f(x,z)$ depends on the value of x. Said another way, a density feedback is present if there is a coupling between the density dynamics and the value of the species density. Mathematically, a feedback is present if $\partial f(x,z)/\partial x \neq 0$ for some range of x. For example, the exponential growth equation $dx/dt = zx$ has a density feedback whereas the growth rate $dx/dt = z$ does not have a

density feedback. Similarly, a phenotype feedback is present if the phenotype dynamics depend on the phenotype of the species, i.e., the phenotype dynamics are coupled ot the value of the phenotype, which mathematically means $\partial g(x,z)/\partial z \neq 0$ for some range of z. The density-phenotype feedback is present if the density and phenotype dynamics depend on the value of the other variable, i.e., $\partial f(x,z)/\partial z \neq 0$ and $\partial g(x,z)/\partial x \neq 0$. In total, the different feedbacks are present/absent depending on whether the dynamics of the variables are coupled, which mathematically can be captured by non-zero derivatives of the equations describing the dynamics.

The strengths of those feedbacks depend on both the strength of the coupling between the variables (i.e., the magnitudes of the partial derivatives in the previous paragraph) and the speeds of the dynamics (i.e., the magnitudes of the rates of change). To see this, without loss of generality we Taylor expand the differential equations about $t = 0$ to get

$$\frac{dx}{dt}(t) = \frac{dx}{dt}(t)\bigg|_{t=0} + \frac{d^2x}{dt^2}(t)\bigg|_{t=0} t + \mathcal{O}(t^2) \tag{S.1}$$

$$= \frac{dx}{dt}(t)\bigg|_{t=0} + \overbrace{\left(\frac{\partial}{\partial x}\frac{dx}{dt}\right)}^{\text{den coupling}} \overbrace{\frac{dx}{dt}\bigg|_{t=0} t}^{\text{density dynamics}} + \overbrace{\left(\frac{\partial}{\partial z}\frac{dx}{dt}\right)}^{\text{den-ph coupling}} \overbrace{\frac{dz}{dt}\bigg|_{t=0} t}^{\text{phenotype dynamics}} + \mathcal{O}(t^2) \tag{S.2}$$

$$= \epsilon_x f|_{t=0} + \overbrace{\epsilon_x^2 \frac{\partial f}{\partial x} f\bigg|_{t=0} t}^{\text{density feedback}} + \overbrace{\epsilon_x \epsilon_z \frac{\partial f}{\partial z} g\bigg|_{t=0} t}^{\text{density-phenotype feedback}} + \mathcal{O}(t^2) \tag{S.3}$$

$$\frac{dz}{dt}(t) = \frac{dz}{dt}(t)\bigg|_{t=0} + \frac{d^2z}{dt^2}(t)\bigg|_{t=0} t + \mathcal{O}(t^2) \tag{S.4}$$

$$= \frac{dz}{dt}(t)\bigg|_{t=0} + \overbrace{\left(\frac{\partial}{\partial x}\frac{dz}{dt}\right)}^{\text{den-ph coupling}} \overbrace{\frac{dx}{dt}\bigg|_{t=0} t}^{\text{density dynamics}} + \overbrace{\left(\frac{\partial}{\partial z}\frac{dz}{dt}\right)}^{\text{ph coupling}} \overbrace{\frac{dz}{dt}\bigg|_{t=0} t}^{\text{phenotype dynamics}} + \mathcal{O}(t^2) \tag{S.5}$$

$$= \epsilon_z g|_{t=0} + \overbrace{\epsilon_x \epsilon_z \frac{\partial g}{\partial x} f\bigg|_{t=0} t}^{\text{density-phenotype feedback}} + \overbrace{\epsilon_z^2 \frac{\partial g}{\partial z} g\bigg|_{t=0} t}^{\text{phenotype feedback}} + \mathcal{O}(t^2) \tag{S.6}$$

We focus on the terms that are linear in t because the higher order terms are smaller for $t \ll 1$. Equation (S.2) shows that the density dynamics depend on (i) how the density dynamics are coupled to the species' density ($\frac{\partial}{\partial x}\frac{dx}{dt}$) and phenotype ($\frac{\partial}{\partial z}\frac{dx}{dt}$) and (ii) the rates of change of the density (dx/dt) and phenotype (dz/dt). Combining those factors defines the density feedback and one component of the density-phenotype feedback. Similarly, equation (S.5) shows that the phenotype dynamics depend on (i) how the phenotype dynamics are coupled to the species' density ($\frac{\partial}{\partial x}\frac{dz}{dt}$) and phenotype ($\frac{\partial}{\partial z}\frac{dz}{dt}$) and (ii) the rates of change of the density (dx/dt) and phenotype (dz/dt). Combining those factors defines the phenotype feedback and the other component of the density-phenotype feedback.

Equations (S.3) and (S.6) show that the strengths of the effect of the density feedback, the density-phenotype feedback, and the phenotype feedback are proportional to ϵ_x^2, $\epsilon_x\epsilon_y$, and ϵ_z^2, respectively. This means that if the coupling between variables is relatively equal, then the strengths of the different feedbacks can often be predicted by the maximum rates of

change of the variables (ϵ_x, ϵ_z). For example, if the phenotype dynamics are much faster than the density dynamics (i.e., $\epsilon_x \ll \epsilon_z$) and the coupling between all variables is comparable (i.e., $\frac{\partial}{\partial x}\frac{dx}{dt}$ and $\frac{\partial}{\partial z}\frac{dx}{dt}$ are similar in magnitude), then the density-phenotype feedback term in equation (S.3) will be much larger than the density feedback term. Thus, while density and density-phenotype feedbacks both affect the population density dynamics, the density-phenotype feedback has a much larger effect because the phenotype dynamics are faster.

We note four things about and related to the above. First, one variable being faster than the other (e.g., $\epsilon_x > \epsilon_z$) does not necessarily imply that the feedbacks involving the faster variable are always larger than the feedbacks involving the slower variable. This is because the strengths of the feedbacks are determined jointly by (i) the maximum rate of change of involved variables (e.g., ϵ_x), (ii) the realized rate of change at that point in time (e.g., $f(x, z)$) and (iii) the coupling between the variables (e.g., $\partial g/\partial x$). For example, the density-phenotype feedback in equation (S.6) may be weaker than the density feedback when the density dynamics are faster than the phenotypic dynamics ($\epsilon_x > \epsilon_z$) if coupling between the phenotype and density is weak ($\partial g/\partial x$, e.g., changes in density have little effect on selection) or if the species density is currently changing slowly ($f \approx 0$ because the system is near the x-nullcline). That being said, if the coupling between all variables is similar in magnitude, then in many regions of parameter space the maximum rates of change will determine which feedbacks are stronger or weaker. This means that identifying faster versus slower variables using maximum rates of change can help identify specific feedbacks that are more likely to have stronger effects than other feedbacks, but that does not imply one feedback has stronger effects than another feedback at all points in time.

Second, the above is directly related to theory in previous studies (Cortez 2018; Patel et al. 2018; Cortez and Patel 2017; Cortez et al. 2020) that have measured the strengths of the effects of different feedbacks on equilibrium stability. In those studies, feedbacks are defined by submatrices of the Jacobian and their determinants. The above equations also depend on the Jacobian (although not evaluated at equilibrium). To see this, we rewrite equations (S.2)-(S.5) as

$$\begin{pmatrix} \frac{dx}{dt}(t) \\ \frac{dz}{dt}(t) \end{pmatrix} = \begin{pmatrix} \frac{dx}{dt}(0) \\ \frac{dz}{dt}(0) \end{pmatrix} + \begin{pmatrix} \frac{\partial}{\partial x}\frac{dx}{dt} & \frac{\partial}{\partial z}\frac{dx}{dt} \\ \frac{\partial}{\partial x}\frac{dz}{dt} & \frac{\partial}{\partial z}\frac{dz}{dt} \end{pmatrix} \begin{pmatrix} x(t) \\ y(t) \end{pmatrix}\Bigg|_{t=0} t + \mathcal{O}(t^2). \tag{S.7}$$

where the 2x2 matrix is the Jacobian of the model.

Third, comparing the maximum rates of density and phenotypic change allows one to make predictions about whether density, density-phenotype, and phenotype feedbacks are more likely to have stronger effects on the system dynamics. However, this does not mean that those feedbacks have the strongest effects on the system dynamics. This is because the densities or phenotypes of other species or other environmental variables may have stronger effects on the dynamics of the system. Nonetheless, even when other variables are affecting the dynamics of the system, comparing maximum rates of change still provides insight into whether the density, density-phenotype, or phenotype feedbacks of a focal species are more likely to have stronger effects on the system dynamics.

To see this, let x and z denote the density and population-level phenotype for a focal species and let $y_i(t)$ $(1 \leq i \leq n)$ denote all other variables in the system. Each $y_i(t)$ could

be the density or trait of another interacting species or some other environmental variable (e.g., temperature). We model this system using the system of differential equations,

$$\begin{aligned}\frac{dx}{dt} &= \epsilon_x f(x, z, y_1, ..., y_n)\\ \frac{dz}{dt} &= \epsilon_z g(x, z, y_1, ..., y_n)\\ \frac{dy_i}{dt} &= \epsilon_i h_i(x, z, y_1, ..., y_n, t), \quad 1 \leq i \leq n.\end{aligned} \tag{S.8}$$

The dynamics of y_i can depend on x and z (e.g., when y_i is the density of an interacting species) or be independent of those variables (e.g., if y_i is temperature then it may only be a function of time, $h_i(t)$). Taylor expanding the dx/dt and dz/dt equations as before yields

$$\begin{aligned}\frac{dx}{dt}(t) = \epsilon_x f|_{t=0} + \overbrace{\epsilon_x^2 \frac{\partial f}{\partial x} f\Big|_{t=0} t}^{\text{density feedback}} + \overbrace{\epsilon_x \epsilon_z \frac{\partial f}{\partial z} g\Big|_{t=0} t}^{\text{density-phenotype feedback}}\\ + \overbrace{\sum_i \epsilon_i \epsilon_x \frac{\partial f}{\partial y_i} h(t)\Big|_{t=0} t}^{\text{other feedbacks and effects}} + \mathcal{O}(t^2)\end{aligned} \tag{S.9}$$

$$\begin{aligned}\frac{dz}{dt}(t) = \epsilon_z g|_{t=0} + \overbrace{\epsilon_x \epsilon_z \frac{\partial g}{\partial x} f\Big|_{t=0} t}^{\text{density-phenotype feedback}} + \overbrace{\epsilon_z^2 \frac{\partial g}{\partial z} g\Big|_{t=0} t}^{\text{phenotype feedback}}\\ + \overbrace{\sum_i \epsilon_i \epsilon_x \frac{\partial g}{\partial y_i} h(t)\Big|_{t=0} t}^{\text{other feedbacks and effects}} + \mathcal{O}(t^2)\end{aligned} \tag{S.10}$$

These equations are same as equations (S.3) and (S.6) except that they account for how the other variables affects the dynamics of the focal species' density and trait.

Importantly, the relative strengths of the density, density-phenotype and phenotype feedbacks involving the focal species' density and trait are unaffected by the dynamics of the additional variables. For example, if the phenotype dynamics of the focal species are much faster than its density dynamics ($\epsilon_z \gg \epsilon_x$) and there is sufficient coupling between the variables, then the effect of the focal species' density-phenotype feedback on the density dynamics of the focal species are stronger than the effects of the focal species' density feedbacks. However, without information about the rates of change of the other variables (y_i) and how the dynamics of the focal species are coupled to them, it is not possible to determine whether the density, density-phenotype, and phenotype feedbacks involving just the focal species are weaker, stronger or comparable to the effects of the feedbacks involving the other variables.

Finally, while the above focuses on feedbacks between two variables, everything extends to feedbacks between any combination of species' densities and population-level traits by adding additional equations and using linear algebra. The mathematics simply involves applying the linear algebra illustrated in equation (S.7) to equations analogous to equations

(S.9) and (S.10) for the appropriate set of variables. For example, the feedbacks involving just x, z and y_1 would be derived by Taylor expanding the dx/dt, dz/dt, and dy_1/dt equations and computing a 3x3 submatrix of the Jacobian. As another example, the feedbacks between all variables in model (S.8) are defined by equation (S.7) where $(x(t), z(t))$ is replaced by $(x(t), z(t), y_1(t), ..., y_n(t))$ (and similarly for the derivatives) and the matrix is the full Jacobian for the model.

S1.2 Details about empirical data sets

The data sets for all analyzed studies are included in the supplementary files uploaded to the Dryad Digital Repository (Grosklos and Cortez 2020). The data from Edeline et al. (2008), Haafke et al. (2016), Hiltunen et al. (2014), Kasada et al. (2014), and Sanchez and Gore (2013) were shared with us by the authors of those studies. The data for all other studies was extracted from published PDFs. One study (Le Galliard et al. 2005) analyzed in the DeLong et al. (2016) study was excluded from our analysis because it was unclear how to compute the total density of the population.

For most studies the population-level trait was the mean value of a quantitative phenotype (e.g., beak size or wing length). For eight of the studies (6 with heritable traits, 2 with an unknown mode of adaptation), the original data consisted of densities or abundances of two different phenotypes (e.g., susceptible and resistant bacterial strains, or red and yellow color morphs). For these systems, we used the frequency of one phenotype as the population-level trait. Specifically, if $a_1, ..., a_n$ and $b_1, ..., b_n$ are the densities of each phenotype at time points $t_1, ..., t_n$, then the total density at each point is $x_i = a_i + b_i$ and the population-level trait is $z_i = a_i/x_i$. Using the proportion of one phenotype as the population-level trait is appropriate for these systems because in any system where individuals can only take on one of two phenotypes, there is a one-to-one mapping between the mean phenotype and the proportion of one phenotype. In particular, if phenotype i has trait value v_i density n_i, then the average trait value can be uniquely written in terms of the proportion of phenotype 1 (p_1) using $(v_1 n_1 + v_2 n_2)/(n_1 + n_2) = v_1 p_1 + v_2(1 - p_1)$. We note that because the clones in the Fenchel and Jonsson (1988) study have different plastic responses to predation, each individual's trait is a reaction norm.

The estimated scaled maximum rates of density and phenotypic change for each published time series are listed in Table S1. Multiple lines for a single study mean that multiple time series from that study were analyzed. The scaled maximum rates listed in Table 1 and plotted in Figure 3A are the averages of those in Table S1. Figure 3B in the main text plots the ratio of the average maximum phenotypic rate and the average maximum density rate, i.e., $\langle \epsilon_{ph} \rangle / \langle \epsilon_{den} \rangle$. The ratio for each individual time series is listed in Table S1 and plotted in Figure S1.

We classify each study as either a field-based study (FS) or a constant condition laboratory experiment (LE); see column Exp in Table S1. Field-based studies involved data collected in a natural setting. Temporal dynamics in these populations were driven by a combination of species interactions and natural environmental forcing (e.g., seasonal forcing). We note that the Campbell and Echternacht (2003) study was unique in that it seeded uninhabited islands with a small number of individuals and observed the population in sub-

sequent years. Laboratory studies involved communities held under constant environmental conditions. For all laboratory studies, the communities were either (i) seeded with populations whose densities and phenotypic distributions were not at equilibrium values or (ii) seeded initially with monomorphic populations and then additional genotypes were introduced at a later point in time. In all cases, the temporal dynamics in these studies are driven by factors internal to the system (e.g., predatory interactions) and not by external environmental forcing.

Because the sampling interval could potentially affect our results, Table S1 also lists the total number of samples for each time series (SS), total time elapsed (Total T), average sampling interval size (Avg SI), and the maximum time between consecutive measurements (Max SI). For some studies, these values differed between the density and trait time series, but because these differences were nominal, we only reported the values for the density time series in Table S1. The average number of samples collected per generation for every study is plotted in Figure S2. There are 17 studies with at least one sample per generation on average. We expect that undersampling is not an issue for these studies. There are 13 studies where the average number of samples is less than one per generation (studies coded by c, j, k, l, m, q, r, B, C, E, F, H, and η), with 4 of those studies (coded by c, j, q, and h) having less than 1 sample per 10 generations on average. As noted in the main text, 6 of the studies (coded j, k, l, m, H, and η) are unlikely to be affected by the sparse sampling because the evolving species is a prey in a predator-prey system and the sampling interval was a small fraction of the predator generation time (which limits the period of the cycles). Undersampling could be affecting the results of the remaining 7 studies (coded by c, q, r, B, C, E, and F). This is less likely for the Caron et al. (1985), DeLong et al. (2014), Gonzalez et al. (1993), and Lürling et al. (2005) studies (coded by B, C, E, and F), which have one sample per 1.4-4 generations on average and maximum gaps between consecutive samples that range between 3.9 and 5.1 generations. Additional evidence of this for DeLong et al. (2014) (coded by C) is provided by the tight fit between the data and mechanistic model in that study; see Figure 1 of that study. Undersampling has a greater likelihood of affecting the results for the other studies (coded by c, q, and r) which have one sample per 4.6-84 generations on average and maximum gaps between consecutive samples that range between 5 and 220 generations.

S1.3 Model simulations

The simulations in Figures 1 and 2 are from the Abrams and Matsuda (1997) model, modified so that the prey density and prey trait equations are multiplied by dimensionless time scale parameters ϵ_x and ϵ_z. This model is,

$$\begin{aligned}
\frac{dx}{dt} &= \epsilon_x \left(rx + qxz - kx^2 - \frac{axyz}{1+hxz} \right) \\
\frac{dy}{dt} &= \frac{caxyz}{1+hxz} - my \\
\frac{dz}{dt} &= \epsilon_z V \left(q - \frac{ay}{1+hxz} \right) e^{-s/(z-s)},
\end{aligned} \tag{S.11}$$

where x is the prey density, y is the predator density, and z is the population-level prey trait (defense). The parameters are: prey attack rate, a, prey to predator density conversion rate, c, predator handling time, h, predator per capita death rate, m, trait-depended prey maximum exponential growth rate, $r + qz$, and prey intraspecific competition coefficient, k. In the trait equation, V is the standing genetic variation and the function $\exp(-s/(z-s))$ bounds the trait above the small value s.

For the simulation in Figure 1, the parameters are $r = 2.5$, $q = 0.8$, $k = 1$, $a = 1$, $h = 1$, $c = 1$, $m = 0.5$, $V = 1$, $s = 0.001$, $\epsilon_x = 1$, and $\epsilon_z = 0.01$ and the initial conditions are $(x, y, z) = (5, 5, 0.5)$. For all panels in Figure 2, the parameters are $r = 0.25$, $q = 0.08$, $k = 0.1$, $a = 0.1$, $h = 1$, $c = 10$, $m = 0.5$, $V = 0.175$, and $s = 0.001$ and the initial conditions are $(x, y, z) = (5, 1, 1.5)$. These values were chosen such that $\epsilon_{ph} \approx \epsilon_{den}$ when estimated from simulations where $\epsilon_x = \epsilon_z = 1$. In panels A-D, the step size for all simulations is 1 time unit, $\epsilon_x = 0.1$ for all simulations, and ϵ_z is set to 2, 1, 0.5, 0.1, and 0.05. Panels E-H use the same parameters as panels A-D, respectively, with step sizes of 1 (black symbols), 4, 10, 20, 40, 100, and 200 (lightest gray symbols) time units.

S1.4 Comparison of results from methods using alternative scalings and summary statistics

We compared the rates of density and phenotypic change estimated using the method in this study, the method in DeLong et al. (2016), and methods that use alternative scalings. The rows of Figure S3 involve different scalings of the rates and the columns of Figure S3 differ in terms of comparing (left) maximum rates and (right) averaged rates. Figure S3A shows the estimated maximum rates of change scaled by the range of the data (and the species generation time, G). Figure S3B shows the estimated maximum rates of change where the derivatives are per capita rates, computed using $|(x_{i+1} - x_i)/(t_{i+1} - t_i)| \cdot (G/x_i)$ and $|(z_{i+1} - z_i)/(t_{i+1} - t_i)| \cdot (G/z_i)$. Figure S3C shows the estimated maximum rates of change of the unscaled rates, computed using $|(x_{i+1} - x_i)/(t_{i+1} - t_i)|$ and $|(z_{i+1} - z_i)/(t_{i+1} - t_i)|$. Figure S3D shows the estimated maximum rates of change scaled by the standard deviation of the time series; this is computed using $|(x_{i+1} - x_i)/(t_{i+1} - t_i)| \cdot (G/\text{std}(x_i))$ and $|(z_{i+1} - z_i)/(t_{i+1} - t_i)| \cdot (G/\text{std}(z_i))$ where $\text{std}(x_i)$ and $\text{std}(z_i)$ are the stand deviations of the density and phenotype time series. Panels E-H show average rates of change scaled in the same way as panels A-D. Figure S3A uses the method from this study and Figure S3F uses the method from DeLong et al. (2016).

When computing per capita rates of change (as in DeLong et al. (2016)), some data points in the time series were omitted because the trait or population density took on a value of 0, which results in a divide by zero error when computing per capita rates. We omitted 1 data point in Becks et al. (2010), 20 data points in Kasada et al. (2014), and 14 data points in Sanchez and Gore (2013).

Comparing Figure S3A,E and Figure S3B,F shows that the key factor driving the different results between our study and DeLong et al. (2016) is the choice of scaling (i.e., scaling by range versus per capita rates). In general, the increased scatter of the data points in Figure S3B,F is due to small divisor issues. Specifically, if the population density (x) is small

in magnitude, then small amounts of variation in x cause large changes in the value of $(1/x)(dx/dt)$; the same applies to when the trait value (z) is small in magnitude. These small divisor issues result in scaled maximum rates of change that are much larger than expected. This in turn results in some studies having maximum or average phenotypic rates that are more than 10 times faster or more than 10 times slower than the corresponding rates of change in density. For example, the placement of data set r (Schrag and Mittler 1996) is caused, in part, by the per capita rate of phenotypic change being massive because the mean phenotype is close to zero. These small divisor issues and the omitted data points in the previous paragraph highlight the perils of using per capita rates when comparing rates of density and phenotypic change.

Comparing Figure S3A,E and Figure S3D,H shows that our results are qualitatively unchanged if the maximum or average rates of change are scaled by the sample standard deviation. Specifically, scaling by sample standard deviation produces maximum phenotypic rates of change that are between 0.4 and 2.5 times faster than maximum density rates of change.

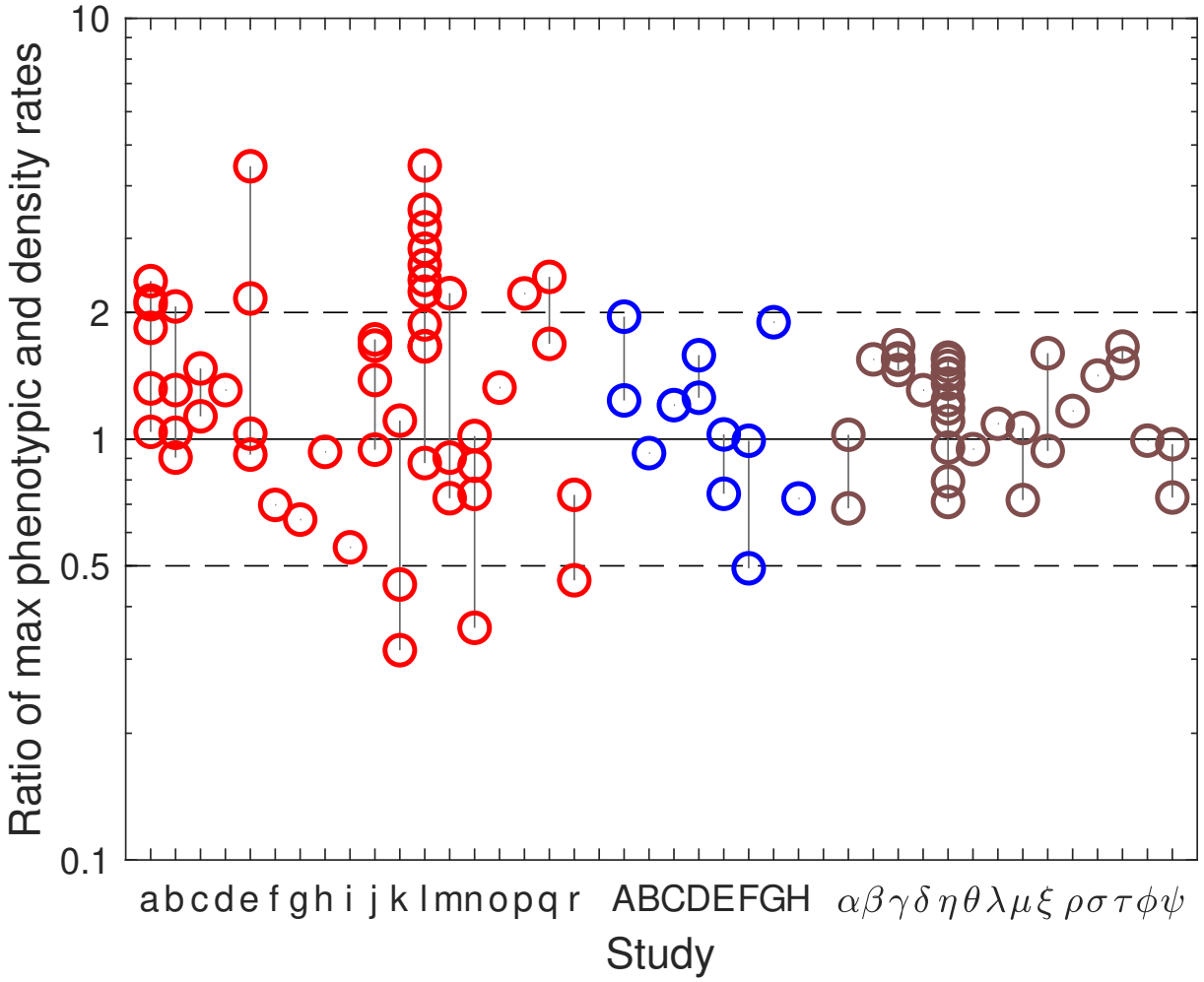

Figure S1: Ratios of maximum phenotypic rates and maximum density rates for all time series analyzed in this study. Replicates from the same study are connected by solid vertical gray lines. Studies are colored according to the mode of adaptation: genetic (a−r; red), plastic (A−H; blue), and unknown ($\alpha - \psi$; brown). Symbols correspond to studies listed in Tables 1 and S1. The horizontal lines denote when phenotypic rates are two times faster (upper dashed line), equal to (solid line), and two times slower (lower dashed line) than density rates of change.

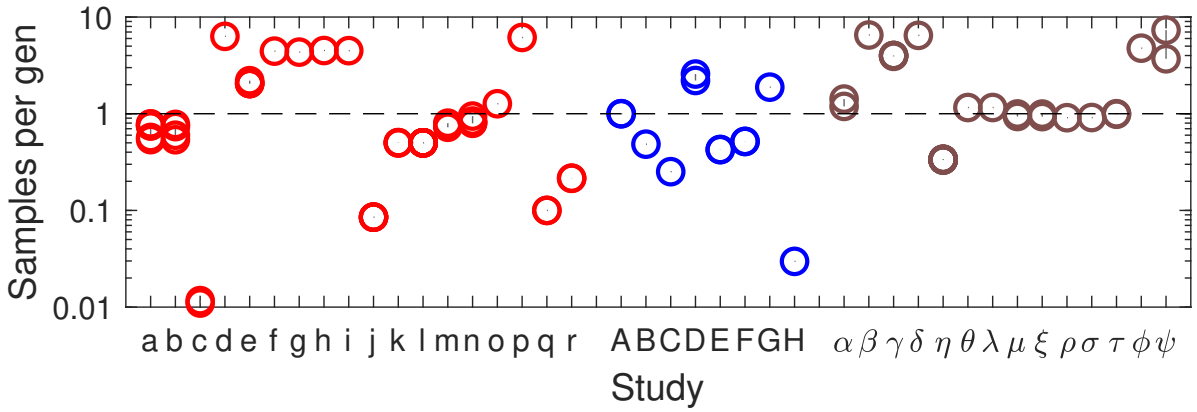

Figure S2: The average number of samples collected per generation for all time series analyzed in this study. Replicates from the same study are connected by solid vertical gray lines. Symbols correspond to studies listed in Tables 1 and S1 and colored according to the mode of adaptation: genetic (a−r; red), plastic (A−H; blue), and unknown ($\alpha - \psi$; brown). The dashed line represent studies where the average number of samples collected were once per generation. Studies that lie below the dashed line indicate that less than one sample was collected per generation.

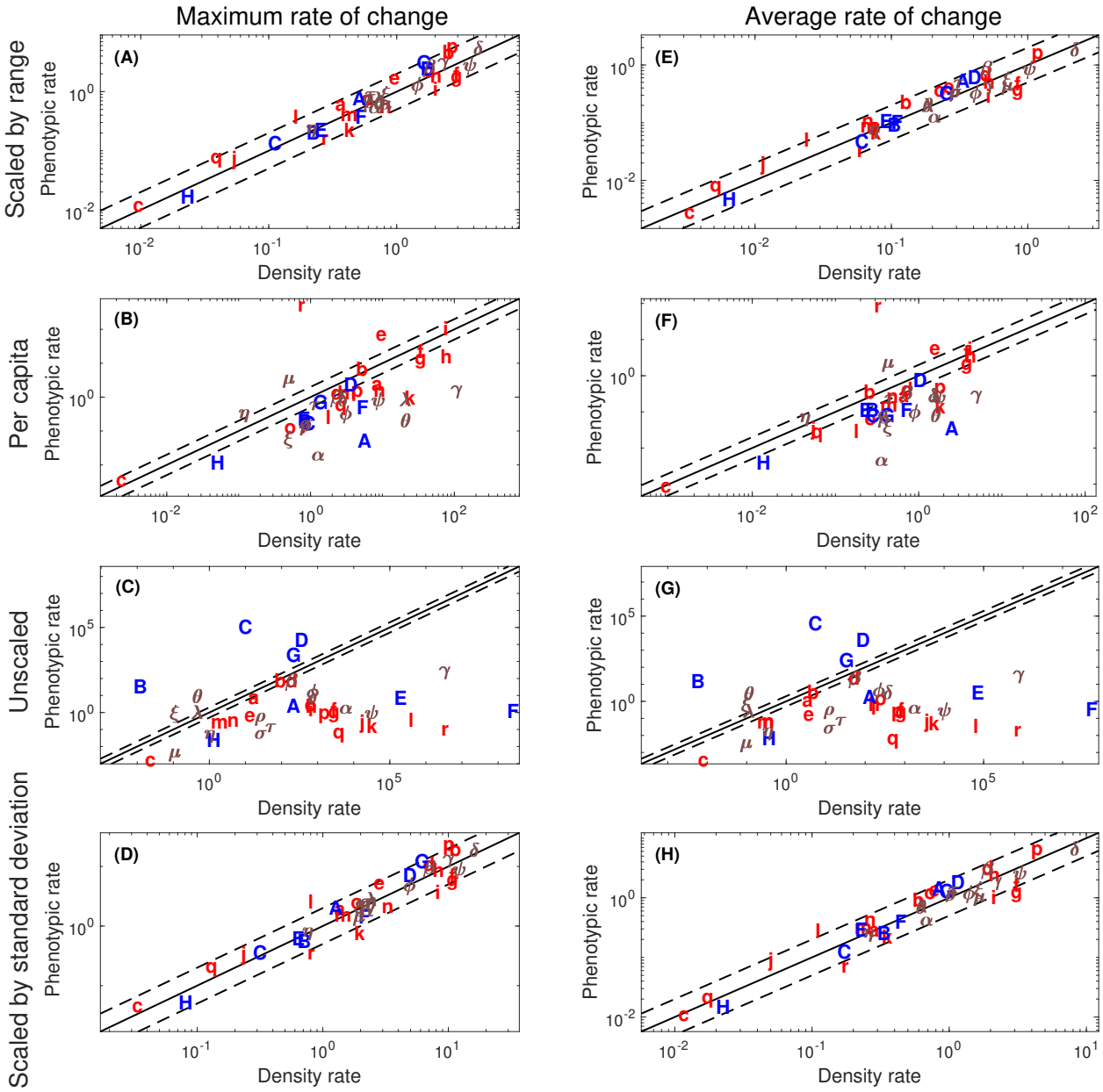

Figure S3: Comparison of the methods for estimating rates of density and phenotypic change used in the current study and in DeLong et al. (2016). Rates of density and phenotypic change estimated (left column) using maximum derivatives or (right column) average derivatives that are either (4th row) scaled by the standard deviation, (3rd row) unscaled, (2nd row) scaled by the magnitude of the values (i.e., per capita rates), or (1st row) scaled by the range of the data. Panel A shows the results from the method used in the current study. Panel F shows the results from the method used in DeLong et al. (2016). In all panels, the black line denotes the 1:1 line and the upper and lower dashed lines denote where phenotypic rates of change are two times faster or two times slower, respectively, than density rates of change. Symbols correspond to studies listed in Table 1.

Table S1: Estimated scaled maximum rates of density and phenotypic change for each time series.

Code	Study	Figure	Trait	Data	Type	ϵ_{den}	ϵ_{ph}	$\epsilon_{ph}/\epsilon_{den}$	SS	Total T	Avg SI	Max SI	Gen	Unit
Genetic														
a	Becks et al. (2010)	4a	Clump size	E	LE	0.3	0.72	2.4	22	21	1	1.3	0.78	days
		4b				0.25	0.46	1.8	26	26	1	2.1		
		4c				0.55	0.58	1	42	43	1	2.2		
		4d				0.41	0.54	1.3	32	31	1	1.2		
		4e				0.34	0.72	2.1	44	59	1.4	2.8		
		4f				0.36	0.75	2.1	42	59	1.4	2.7		
b	Becks et al. (2012)	1a	Clump size	E	LE	0.39	0.4	1	79	101	1.3	3.6	0.78	days
		1b				8.6	18	2.1	79	114	1.5	3.5		
		1c				0.32	0.42	1.3	46	47	1	2		
		1d				0.83	0.75	0.9	74	73	1	1.7		
c	Bohannon and Lenski (1998)	2a	Proportion susceptible	E	LE	0.011	0.012	1.1	19	385	21	55	0.25	hrs
		2b				0.0086	0.013	1.5	18	386	23	55		
d	Coltman et al. (2003)	2b, 2c	Horn length (adult male)	E	FS	1.8	2.4	1.3	31	30	1	1.1	6	yrs
e	Fussman et al. (2003)	2a	Proportion mictic (female)	E	LE	1.4	1.3	0.92	25	25	1.1	1.5	2.2	days
		2b				0.71	1.5	2.2	25	26	1.1	2		
		2c				1	1.1	1	25	26	1.1	1.5		
		2d				0.74	3.3	4.5	25	26	1.1	1.9		
f	Grant and Grant (2002)	5a, 1b	*G. fortis* Beak length	E	FS	2.9	2.1	0.7	30	29	1	1.1	4.5	yrs
g		5a, 1e	*G. fortis* Beak shape			2.9	1.9	0.64	30	29	1	1.1		
h	Grant and Grant (2002)	5a, 1c	*G. scandens* Beak length	E	FS	2	1.9	0.93	30	29	1	1.1	4.5	yrs
i		5a, 1f	*G. scandens* Beak shape			2	1.1	0.55	30	29	1	1.1		
j	Haafke et al. (2016)	3E(top)	Clump size	O	LE	0.065	0.062	0.94	80	102	1.3	22	0.11	wks
		3E(bottom)				0.053	0.074	1.4	80	102	1.3	22		
		S7A				0.053	0.092	1.7	80	102	1.3	22		
		S7B				0.046	0.077	1.7	80	102	1.3	22		
k	Hiltunen and Becks (2014)	2b, 2e	Proportion defended	E	LE	0.54	0.17	0.32	15	28	2	2.1	1	days
		2c, 2f				0.48	0.22	0.45	15	28	2	2.1		
		2d, 2g				0.27	0.3	1.1	15	28	2	2.1		
l	Hiltunen et al. (2014)	2.3a, 2.3b	Clump size	O	LE	0.19	0.17	0.88	177	176	1	1	0.5	days
		2.3e, 2.3f				0.21	0.35	1.7	223	222	1	1		
		2.3g, 2.3h				0.17	0.39	2.2	157	157	1	2		
		2.4a, 2.4b				0.13	0.42	3.2	185	184	1	1		
		2.4c, 2.4d				0.16	0.46	2.8	190	189	1	1		
		2.4e, 2.4f				0.21	0.5	2.4	186	186	1	2		
		2.4g, 2.4h				0.21	0.39	1.9	66	65	1	1		
		2.5a, 2.5b				0.18	0.29	1.7	190	189	1	1		
		2.5e, 2.5f				0.11	0.38	3.5	24	23	1	1		
		2.5c, 2.5d				0.095	0.43	4.5	187	186	1	1		
		2.5g, 2.5h				0.15	0.38	2.6	66	65	1	1		

Columns are the study code (a−r for genetic traits, A−H for plastic traits, and $\alpha - \psi$ for unknown) whether the data was extracted from PDF (E) or obtained from authors of the study (O), experiment type (Exp), calculated maximum rates of density (ϵ_{den}) and phenotypic (ϵ_{ph}) change and their ratio ($\epsilon_{ph}/\epsilon_{den}$), sample size (SS), total time elapsed (Tot T), average sampling interval size (Avg SI), maximum sampling interval size (Max SI), generation time (Gen), and time unit (Unit). Multiple rows for the same study correspond to different replicates.

*The density data is from Figure 1a of Ezard et al. (2009) and the phenotypic data is from Figure 1c of Ozgul et al. (2009).

Table S1 (continued)

Code	Study	Figure	Trait	Data	Type	ϵ_{den}	ϵ_{ph}	$\epsilon_{ph}/\epsilon_{den}$	SS	Total T	Avg SI	Max SI	Gen	Unit
m	Kasada et al. (2014)	2A,B	Proportion defended (costly tradeoff)	O	LE	0.17	0.38	2.2	43	58	1.4	4	1	days
		2C,D				0.48	0.43	0.9	54	69	1.3	4.7		
		2E,F				0.64	0.47	0.72	33	40	1.3	4		
n		3A,B	Proportion defended (cheap tradeoff)			1.1	0.39	0.36	57	59	1.1	3		
		3C,D				0.72	0.74	1	54	63	1.2	3		
		3E,F				0.68	0.59	0.86	59	72	1.2	3.4		
		3G,H				0.78	0.58	0.74	56	69	1.3	3.4		
o	Milot et al. (2011)	S1, 2	Age at first reproduction	E	FS	0.58	0.77	1.3	8	149	21	31	27	yrs
p	Robinson et al. (2006)	2	Proportion normal horned	E	FS	2.7	6.1	2.2	18	18	1.1	2	6.5	yrs
q	Sanchez and Gore (2013)	2b	Proportion cooperator	O	LE	0.041	0.1	2.4	5	6	1	1	0.1	days
		2c				0.037	0.063	1.7	7	6	1	1		
r	Schrag and Mittler (1996)	5a	Proportion resistant	E	LE	0.29	0.21	0.74	7	8	1.3	2.3	0.283	hrs
		5b				0.26	0.12	0.46	7	8	1.3	2.3		
Plastic														
A	Campbell and Echternacht (2003)	3, Table 2	Snout-vent length	E	FS	0.61	0.76	1.2	4	3	0.99	0.99	1	yrs
		3, Table 2				0.42	0.81	2	4	3	0.99	0.99		
B	Caron et al. (1985)	6	Cell volume	E	LE	0.22	0.21	0.93	9	4	0.51	1.1	0.25	days
C	DeLong et al. (2014)	1b, 1d	Cell volume	E	LE	0.11	0.14	1.2	9	8	0.98	1.2	0.25	days
D	Fenchel and Jonsson (1988)	2a	Cell volume	E	LE	1.9	3.1	1.6	15	115	8.2	40	12	hrs
		2b				1.5	1.9	1.3	15	73	5.2	16		
E	Gonzalez et al. (1993)	1a, 1b	Cell volume	E	LE	0.28	0.2	0.74	8	164	23	51	10	hrs
		1a, 1b				0.24	0.24	1	8	165	24	52		
F	Lürling et al. (2005)	1A, 2	Clump size	E	LE	0.55	0.27	0.49	36	50	1.4	3.2	1	days
		1A, 2				0.51	0.5	0.99	47	64	1.4	3.9		
G	Ozgul et al. (2010)	1b, 1c	Weight	E	FS	1.7	3.1	1.9	31	32	1.1	1.9	2	yrs
H	Suzuki et al. (2017)	3a, 3c	Cell volume	E	LE	0.023	0.017	0.72	20	32	1.7	3	0.05	days
Unknown														
α	Brown and Brown (2013)	1a, 1c	Wing length (nest)	E	FS	0.69	0.47	0.68	30	29	1	1.2	1.5	yrs
		1a, 1c	Wing length (roadkill)		FS	0.69	0.71	1	25	29	1.2	4		
β	Coltman et al. (2003)	2a, 2c	Weight (adult male)	E	FS	1.8	2.8	1.5	31	30	1	1.1	6	yrs
γ	Edeline et al. (2008)	1c, 1d	Body length	O	FS	2.2	3.5	1.5	51	50	1	1	4	yrs
		1c, 1d				2.2	3.7	1.7	51	50	1	1		
		1c, 1d				2.4	3.7	1.6	51	50	1	1		
		1c, 1d				2.4	3.5	1.5	51	50	1	1		
δ	Ezard et al. (2009)	1a, Ozgul 1c	Weight	E	FS	4.3	5.6	1.3	16	15	1	1.1	6.5	yrs

Table S1 (continued)

Code	Study	Figure	Trait	Data	Type	ϵ_{den}	ϵ_{ph}	$\epsilon_{ph}/\epsilon_{den}$	SS	Total T	Avg SI	Max SI	Gen	Unit
η	Fischer et al. (2014)	D2	Proportion strain 1	E	LE	0.27	0.33	1.2	16	35	2.3	3.1	0.78	days
		D2				0.18	0.28	1.6	16	35	2.3	3.1		
		D2				0.23	0.25	1.1	16	35	2.3	3		
		D2				0.24	0.28	1.2	16	35	2.3	3.1		
		D2				0.21	0.32	1.5	16	35	2.3	3.1		
		D2				0.21	0.2	0.95	16	35	2.3	3.1		
		D2				0.18	0.28	1.5	16	34	2.3	3		
		D2				0.3	0.42	1.4	16	35	2.3	3.2		
		D2				0.15	0.2	1.4	16	35	2.3	3		
		D2				0.22	0.17	0.79	16	35	2.3	3.1		
		D2				0.22	0.31	1.4	16	35	2.3	3		
		D2				0.25	0.18	0.71	16	35	2.3	3.1		
θ	Nakazawa et al. (2007)	2b, 3a	Body length	E	FS	0.72	0.69	0.95	28	27	1	1.2	1.25	yrs
λ		2b, 3b	Wet weight			0.72	0.79	1.1	28	27	1	1.2		
μ	Schoener et al. (2002)	5A, 8	Hindlimb length	E	FS	1	0.72	0.72	3	2	0.99	0.99	1	yrs
		5A, 8				0.62	0.66	1.1	3	2	1	1		
ξ		5A, 8	Lamellae number			1	0.94	0.94	3	2	0.99	0.99		
		5A, 8				0.62	0.99	1.6	3	2	1	1		
ρ	Sinervo et al. (2000)	1d, 1c	Clutch size	E	FS	0.62	0.72	1.2	10	9	1	1.1	1	yrs
σ		1d, 1e	Egg mass			0.62	0.87	1.4	10	9	1	1.1		
τ		1d, 1f	Proportion orange-throated (female)			0.6	0.99	1.7	11	10	0.99	1		
		1d, 1f				0.62	0.93	1.5	10	9	1	1.1		
ϕ	Swain et al. (2007)	1	Body length at age 6 years	E	FS	1.5	1.4	0.99	40	33	0.85	1.9	4.5	yrs
ψ	Tessier et al. (1992)	1a, 5b	Body size	E	FS	2.7	2.7	0.97	17	81	5.1	15	30	days
		1b, 5b				4.7	3.4	0.73	20	78	4.1	9.1		

References

Abrams, P. A., and H. Matsuda. 1997. Prey adaptation as a cause of predator-prey cycles. Evolution 51:1742–1750.

Becks, L., S. Ellner, L. E. Jones, and N. G. Hairston Jr. 2012. Reduction of adaptive genetic diversity radically alters eco-evolutionary community dynamics. Ecology Letters 13:989–997.

Becks, L., S. P. Ellner, L. E. Jones, and N. G. Hairston Jr. 2010. The functional genomics of an eco-evolutionary feedback loop: linking gene expression, trait evolution, and community dynamics. Ecology Letters 15:492–501.

Bohannon, B. J. M., and R. E. Lenski. 1998. Effect of prey heterogeneity on the response of a model food chain to resource enrichment. American Naturalist 153:73–82.

Brown, C. R., and M. B. Brown. 2013. Where has all the road kill gone? Current Biology 23:R233–R234.

Campbell, T., and A. Echternacht. 2003. Introduced species as moving targets: changes in body sizes of introduced lizards following experimental introductions and historical invasions. Biological Invasions 5:193–212.

Caron, D. A., J. C. Goldman, O. K. Andersen, and M. R. Dennett. 1985. Nutrient cycling in a microflagellate food chain: Ii. population dynamics and carbon cycling. Marine Ecology Progress Series 24:243–254.

Coltman, D. W., P. O'Donoghue, J. T. Jorgenson, J. T. Hogg, C. Strobeck, and M. Festa-Bianchet. 2003. Undesirable evolutionary consequences of trophy hunting. Nature 426:655–658.

Cortez, M. H. 2018. Genetic variation determines which feedbacks drive and alter predator-prey eco-evolutionary cycles. Ecological Monographs 88:353–371.

Cortez, M. H., and S. Patel. 2017. The effects of predator evolution and genetic variation on predator-prey population-level dynamics. Bulletin of Mathematical Biology 79:1510–1538.

Cortez, M. H., S. Patel, and S. J. Schreiber. 2020. Destabilizing evolutionary and eco-evolutionary feedbacks drive empirical eco-evolutionary cycles. Proceedings of the Royal Society B 287:20192298.

DeLong, J. P., V. E. Forbes, N. Galic, J. P. Gibert, R. G. Laport, J. S. Phillips, and J. M. Vavra. 2016. How fast is fast? Eco-evolutionary dynamics and rates of change in populations and phenotypes. Ecology and Evolution 6:573–581.

DeLong, J. P., T. C. Hanley, and D. A. Vasseur. 2014. Predator–prey dynamics and the plasticity of predator body size. Functional Ecology 28:487–493.

Edeline, E., T. B. Ari, L. A. Vø llestad, I. J. Winfiled, J. M. Fletcher, J. B. James, and N. C. Stenseth. 2008. Antagonistic selection from predators and pathogens alters food-web structure. PNAS 105:19792–19796.

Ezard, T. H. G., S. D. Cô té, and F. Pelletier. 2009. Eco-evolutionary dynamics: disentangling phenotypic, environmental and population fluctuations. Philosophical Transactions of the Royal Society B 364:1491–1498.

Fenchel, T., and P. R. Jonsson. 1988. The functional biology of strombidium sulcatum, a marine oligotrich ciliate (ciliophora, oligotrichina). Marine Ecology Progress Series 48:1–15.

Fischer, B. B., M. Kwiatkowski, M. Ackermann, J. Krismer, S. Roffler, M. J. Suter, R. I. Eggen, and B. Matthews. 2014. Phenotypic plasticity influences the eco-evolutionary dynamics of a predator–prey system. Ecology 95:3080–3092.

Fussman, G. F., S. P. Ellner, and N. G. Hairston Jr. 2003. Evolution as a critical component of plankton dynamics. Proceedings of the Royal Society of London B 270:1015–1022.

Gonzalez, J. M., E. Sherr, and B. F. Sherr. 1993. Differential feeding by marine flagellates on growing versus starving, and on motile versus nonmotile, bacterial prey. Marine Ecology Progress Series 102:257–267.

Grant, P. R., and B. R. Grant. 2002. Unpredictable evolution in a 30-year study of Darwin's finches. Science 296:707–711.

Grosklos, G., and M.H.. Cortez. 2020. Data from: Evolutionary and plastic phenotypic change can be just as fast as changes in population densities. American Naturalist, Dryad Digital Repository, http://doi.org/10.5061/dryad.b5mkkwhb3 .

Haafke, J., M. A. Chakra, and L. Becks. 2016. Eco-evolutionary feedback promotes Red Queen dynamics and selects for sex in predator populations. Evolution 70:641–652.

Hiltunen, T., and L. Becks. 2014. Consumer co-evolution as an important component of the eco-evolutionary feedback. Nature Communications 5:1–8.

Hiltunen, T., S. P. Ellner, G. Hooker, L. E. Jones, and N. G. Hairston Jr. 2014. Eco-evolutionary dynamics in a three-species food web with intraguild predation: intriguingly complex. Advances in Ecological Research 50:41–73.

Kasada, M., M. Yamamichi, and T. Yoshida. 2014. Form of an evolutionary tradeoff affects eco-evolutionary dynamics in a predator-prey system. PNAS 111:16035–16040.

Le Galliard, J.-F., P. S. Fitze, R. Ferrière, and J. Clobert. 2005. Sex ratio bias, male aggression, and population collapse in lizards. PNAS 102:18231–18236.

Lürling, M., H. Arends, W. Beekman, M. Vos, I. Van der Stap, W. Mooij, and M. Scheffer. 2005. Effect of grazer-induced morphological changes in the green alga scenedesmus obliquus on growth of the rotifer brachionus calyciflorus. Internationale Vereinigung für theoretische und angewandte Limnologie: Verhandlungen 29:698–703.

Milot, E., F. M. Mayer, D. H. Nussey, M. Boisvert, F. Pellletier, and D. Ré ale. 2011. Evidence for evolution in response to natural selection in a contemporary human population. PNAS 108:17040–17045.

Nakazawa, T., N. Ishida, M. Kato, and N. Yamamura. 2007. Larger body size with higher predation rate. Ecology of Freshwater Fish 16:362–372.

Ozgul, A., D. Z. Childs, M. K. Oli, K. B. Armitage, D. T. Blumstein, L. E. Olson, S. Tuljapurkar, and T. Coulson. 2010. Coupled dynamics of body mass and population growth in response to environmental change. Nature 466:482.

Ozgul, A., S. Tuljapurkar, T. G. Benton, J. M. Pemberton, T. H. Clutton-Brock, and T. Coulson. 2009. The dynamics of phenotypic change and the shrinking sheep of St. Kilda. Science 325:464–467.

Patel, S., M. H. Cortez, and S. J. Schreiber. 2018. Partitioning the effects of eco-evolutionary feedbacks on community stability. American Naturalist 191:381–394.

Robinson, M. R., J. G. Pilkington, T. H. Clutton-Brock, J. M. Pemberton, and L. E. B. Kruuk. 2006. Live fast, die young: trade-offs between fitness components and sexually antagonistic selection on weaponry in soay sheep. Evolution 60:2168–2181.

Sanchez, A., and J. Gore. 2013. Feedback between population and evolutionary dynamics determines the fate of social microbial populations. PLoS Biology 11:e1001547.

Schoener, T. W., D. A. Spiller, and J. B. Losos. 2002. Predation on a common anolis lizard: can the food-web effects of a devastating predator be reversed? Ecological Monographs 72:383–407.

Schrag, S. J., and J. E. Mittler. 1996. Host-parasite coexistence: the role of spatial refuges in stabilizing bacteria-phage interactions. American Naturalist 148:348–377.

Sinervo, B., E. Svensson, and T. Comendant. 2000. Density cycles and an offspring quantity and quality game driven by natural selection. Nature 406:985–988.

Suzuki, K., Y. Yamauchi, and T. Yoshida. 2017. Interplay between microbial trait dynamics and population dynamics revealed by the combination of laboratory experiment and computational approaches. Journal of Theoretical Biology 419:201–210.

Swain, D. P., A. F. Sinclair, and J. M. Hanson. 2007. Evolutionary response to size-selective mortality in an exploited fish population. Proceedings of the Royal Society B: Biological Sciences 274:1015–1022.

Tessier, A., A. Young, and M. Leibold. 1992. Population dynamics and body-size selection in *Daphnia*. Limnology and Oceanography 37:1–13.